



January 2017

# On The Development Of Novel Multifunctional Max Reinforced Metals (MRMS) Matrix Composites

Faisal Ahmed Alanazi

Follow this and additional works at: <https://commons.und.edu/theses>

---

## Recommended Citation

Alanazi, Faisal Ahmed, "On The Development Of Novel Multifunctional Max Reinforced Metals (MRMS) Matrix Composites" (2017). *Theses and Dissertations*. 2155.  
<https://commons.und.edu/theses/2155>

This Thesis is brought to you for free and open access by the Theses, Dissertations, and Senior Projects at UND Scholarly Commons. It has been accepted for inclusion in Theses and Dissertations by an authorized administrator of UND Scholarly Commons. For more information, please contact [zeinebyousif@library.und.edu](mailto:zeinebyousif@library.und.edu).

**ON THE DEVELOPMENT OF NOVEL MULTIFUNCTIONAL MAX  
REINFORCED METALS (MRMs) MATRIX COMPOSITES**

by

Faisal Ahmed AlAnazi

Bachelor of Science, King Fahd University of Petroleum and Minerals, Dhahran, 2010

A Thesis

Submitted to the Graduate Faculty

of the

University of North Dakota

In partial fulfillment of the requirements

for the degree of

Master of Science

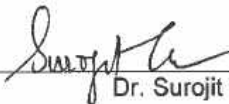
Grand Forks, North Dakota

August

2017

Copyright © 2017 Faisal Ahmed AlAnazi

This thesis, submitted by Faisal Ahmed AlAnazi in partial fulfillment of the requirements for the Degree of Master of Science from the University of North Dakota, has been read by the Faculty Advisory Committee under whom the work has been done and is hereby approved.

  
\_\_\_\_\_  
Dr. Surojit Gupta, Ph. D.

  
\_\_\_\_\_  
Dr. Matthew Cavalli, PhD., P.E.

  
\_\_\_\_\_  
Dr. Clement Tang, Ph.D.

This thesis meets the standards for appearance, conforms to the style and format requirements of the Graduate School of the University of North Dakota, and is hereby approved.

  
\_\_\_\_\_  
Grant McGimpsey  
Dean of the Graduate School

*June 7, 2017*  
\_\_\_\_\_  
Date

## **PERMISSION**

Title            On the Development of Novel Multifunctional MAX Reinforced Metals  
(MRMs) Matrix Composites

Department    Mechanical Engineering

Degree            Master of Science

In presenting this thesis in fulfillment of the requirements for a graduate degree from the University of North Dakota, I agree that the library of this University shall make it freely available for inspection. I further agree that permission for extensive copying for scholarly purposes may be granted by the professor who supervised my thesis work or, in his absence, by the chairperson of the department or the dean of the School of Graduate Studies. It is understood that any copying or publication or other use of this thesis or part thereof for financial gain shall not be allowed without my written permission. It is also understood that due recognition shall be given to me and to the University of North Dakota in any scholarly use which may be made of any material in my thesis.

Signature    Faisal Ahmed AlAnazi

Date 06/08/2017

## TABLE OF CONTENTS

LIST OF FIGURES.....	viii
LIST OF TABLES.....	x
ACKNOWLEDGEMENTS.....	xi
ABSTRACT .....	xii
CHAPTER	
I.    INTRODUCTION.....	1
1.1 Solid Lubricants.....	1
1.2 MAX Phase .....	2
1.3 Introduction MAX Reinforced Metals (MRMs) .....	5
1.4 Current Research Effort .....	9
II.   Synthesis and Tribological Behavior of Novel Wear Resistant Ag and Bi based MRMs (MAX Reinforced Metals) .....	10
2.0 Abstract.....	10
2.1 Introduction.....	11
2.2 Experimental Methods.....	11
2.3 Result and Discussion .....	15
2.3.1 Microstructure and Phase Analysis .....	15
2.3.2 Mechanical Performance .....	19
2.3.3 Tribological Behavior .....	21

2.3.4 Mechanism of Wear .....	28
2.4 Conclusion .....	31
III. Synthesis and Tribological Behavior of Bi-Cr <sub>2</sub> AlC Composites .....	32
3.0 Abstract.....	32
3.1 Introduction.....	33
3.2 Experimental Methods.....	33
3.3 Result and Discussion.....	36
3.3.1 Microstructure and Phase Analysis .....	36
3.3.2 Mechanical Performance .....	38
3.3.3 Tribological Behavior.....	39
3.4 Conclusion .....	41
IV. Synthesis and Tribological Behavior of Al-V <sub>2</sub> AlC, Al-Ti <sub>3</sub> SiC <sub>2</sub> and Al-Cr <sub>2</sub> AlC Composites .....	42
4.1 Introduction.....	43
4.2 Experimental Methods.....	44
4.3 Result and Discussion.....	46
4.4 Conclusion.....	51
V. Conclusion and Future Scope .....	53
4.1 Conclusion.....	53
4.2 Future Scope .....	54
APPENDIX.....	56
REFERENCES.....	56

Chapter I.....	56
Chapter II.....	57
Chapter III.....	59
Chapter IV.....	60



## LIST OF FIGURES

Figure	Page
1.1. Possible combinations of MAX phases.....	3
1.2. Unit Cell for 211(a), 312 (b) and 413 (c) series of MAX phases.....	4
1.3. Tribological performance of MAX phases at room temperature .....	6
1.4. Compressive Strength of Sn-Ti <sub>3</sub> SiC <sub>2</sub> composites .....	7
1.5. Summary of Compressive Strength of different MRM composites .....	7
1.6. Tribological performances of different MRM composite .....	8
2.1. SEM of (a) Bi in SE, (b) Bi-5 vol% Ti <sub>3</sub> SiC <sub>2</sub> , (c) Bi-10 vol% Ti <sub>3</sub> SiC <sub>2</sub> , (d) higher magnification of the marked region in (c), (d) Bi-20 vol% Ti <sub>3</sub> SiC <sub>2</sub> , and (e) Bi-30 vol% Ti <sub>3</sub> SiC <sub>2</sub> in BSE. ....	16
2.2. SEM BSE images of, (a) Ag, (b) Ag-5 vol% Ti <sub>3</sub> SiC <sub>2</sub> , (c) Ag-10 vol% Ti <sub>3</sub> SiC <sub>2</sub> , (d) higher magnification of the marked region in (c), (e) Ag-20 vol% Ti <sub>3</sub> SiC <sub>2</sub> , and (f) Ag-30 vol% Ti <sub>3</sub> SiC <sub>2</sub> composites .....	17
2.3. SE SEM micrographs of etched surfaces of (a) Bi, (b) Bi-20 vol% Ti <sub>3</sub> SiC <sub>2</sub> , (c) Ag, and (d) Ag-20 vol% Ti <sub>3</sub> SiC <sub>2</sub> . ....	18
2.4. Plot of XRD patterns of (a) Bi-based MRMs, and (b) Ag-based MRMs. ....	18
2.5. Plots of variation of (a) porosity, and (b) hardness versus Ti <sub>3</sub> SiC <sub>2</sub> additions. ....	19
2.6. Plot of stress versus displacement of (a) Bi MRMs, (b) Ag MRMs, and (c) yield strength of different MRMs versus Ti <sub>3</sub> SiC <sub>2</sub> additions .....	20
2.7. Plot of friction coefficient ( $\mu$ ) versus distance of (a) Bi-based MRMs, and (b) Ag-based MRMs. ....	22
2.8. Plot of, (a) $\mu_{\text{mean}}$ , and (b) WR as a function of Ti <sub>3</sub> SiC <sub>2</sub> content for different MRMs. ....	23

2.9. SE SEM micrographs of (a) Bi surface, (b) BSE of the same region, (c) alumina counter surface, (d) BSE of the same region, (e) Bi-20 vol% $Ti_3SiC_2$ surface, (f) BSE of the same region, (g) alumina countersurface, and (h) BSE of the same region (inset shows the higher magnification of the marked region) after tribological testing. ....	27
2.10 SE SEM micrographs of (a) Ag-20 vol% $Ti_3SiC_2$ surface, (b) BSE of the same region, (c) alumina countersurface, and (d) BSE of the same region. ....	28
2.11 Schematics of (a1) tribocontact, (a2) Type IVa tribofilm, and (a3) SEM micrograph showing a Type IVa tribofilm formed on alumina surface [2, 28]; (b1) tribocontact, (b2) Type IVb tribofilm [2, 28], and (b3) Type IVb tribofilm formed on alumina surface [28.]; and (c1) tribocontact, (c2) Type IVc tribofilm, and (c3) Type IVc tribofilm formed on alumina surface. ....	30
3.1. SEM SE microstructure of, (a) Bi-10% $Cr_2AlC$ , (b) Bi-20% $Cr_2AlC$ , and (c) Bi-30% $Cr_2AlC$ . ....	37
3.2. Plot of (a) hardness, and (b) porosity versus MAX content. ....	37
3.3. Plot of (a) compressive stress versus displacement, and (b) yield strength versus MAX phase content of different Bi-MAX composites. ....	38
3.4. Plot of (a) friction coefficient, and (b) wear rate versus MAX phase additions. ....	40
3.5. Plot SEM SE micrographs of (a) Bi-20% $Cr_2AlC$ , (b) alumina surface, and (c) BSE image of the same region after tribological testing. ....	41
4.1. Plot of porosity versus MAX phase content .....	46
4.2. Plot of hardness versus MAX phase content .....	47
4.3. Plot of compressive stress versus displacement, (a) Al- $V_2AlC$ , (b) Al- $Ti_3SiC_2$ , (c) Al- $Cr_2AlC$ .	48
4.4. Plot of yield strength versus MAX phase content of different Al-MAX phase composites ..	49
4.5. Plot of friction coefficient versus MAX phase additions .....	50
4.6. Plots of wear rate versus MAX phase additions .....	51

## LIST OF TABLES

Table 2.1: Comparison of tribological behavior of different Ag-based composites .....	25
Table 2.2: Tribochemistry of Different Tribocouples .....	26
Table 4.1: Compositions Table .....	45

## **ACKNOWLEDGEMENTS**

I would like to thank my family for their support, love and patience during my absence. Also, I'm very grateful to my advisor Dr. Surojit Gupta for all the support and guidance that I received during my study. In addition, I would like to thank my sponsor, Saudi ARAMCO, for supporting me during my study.

## ABSTRACT

This work illustrates the synthesis and characterization of novel MAX reinforced metals (MRMs) composites. These composites were tested for their mechanical and tribological performance in ambient temperature. Synthesis and characterization of Bi-Ti<sub>3</sub>SiC<sub>2</sub> and Ag-Ti<sub>3</sub>SiC<sub>2</sub> was studied in Chapter 2. Both composites showed an enhancement in their mechanical and tribological behavior. For example, the addition of 20% Ti<sub>3</sub>SiC<sub>2</sub> decreased the wear rate (WR) by ~12 times in Ag and ~33 times in Bi comparing with the pristine metal. In Chapter 3, Bi-Cr<sub>2</sub>AlC composites were studied and results had been compared to Bi-Ti<sub>3</sub>SiC<sub>2</sub> composites. The addition of 10 vol% Cr<sub>2</sub>AlC was able to decrease the WR of Bi-composites by ~100 times as compared to the Bi metal. Chapter 4 reports the current progress of synthesis and tribological behavior of Al-V<sub>2</sub>AlC, Al-Ti<sub>3</sub>SiC<sub>2</sub> and Al-Cr<sub>2</sub>AlC composites. The addition of MAX phase particulates enhanced the hardness and compressive yield strength of all the compositions. Al-V<sub>2</sub>AlC, Al-Ti<sub>3</sub>SiC<sub>2</sub> and Al-Cr<sub>2</sub>AlC exhibit better tribological behavior compared with pure Al. The WR decreased significantly from 0.25 mm<sup>3</sup>/N.m to 1.1 X 10<sup>-3</sup> mm<sup>3</sup>/N.m in Al-30%V<sub>2</sub>AlC. Similarly, the addition of Ti<sub>3</sub>SiC<sub>2</sub> decreased the WR to 7.3 X 10<sup>-4</sup> mm<sup>3</sup>/N.m in the Al-10%Ti<sub>3</sub>SiC<sub>2</sub>. In Chapter 5, comprehensive conclusion of this thesis and the future scope of study is discussed. Briefly, the addition of MAX phases has beneficial effects on the mechanical and the tribological behavior. However, there is an optimum concentration where the best results are found. That is mainly due to the nature of these phases where they perform much better at higher temperatures rather than room temperature.

# CHAPTER I

## INTRODUCTION

### 1.1 Solid Lubricants

Lubricants, generally in the form of liquid or grease, are used to lower friction and minimize wear rate [1]. However, lubricant properties vary greatly under different service conditions which cause severe deterioration of properties and failure if service parameters were not maintained properly. For example, most liquid lubricants evaporate under vacuum environment whereas solid lubricants can perform outstandingly in vacuum services since they usually have a very low vapor pressure. On the other hand, changes in temperature lead to change in the state of liquid lubricants where liquids may solidify at low temperatures and decompose or oxidize at high temperatures [1]. Furthermore, the heat generated could differ based on the viscosity and whether the liquid follows a shear thinning or shear thickening phenomena. Except for soft metals, most solid lubricants are lacking the ability to carry away the heat that is generated from sliding surfaces since they have a low thermal conductivity. Furthermore, solid lubricants show quite higher friction coefficient and sometimes significant fluctuating of friction. However, this is truly dependent on test environment and applied conditions, e.g. graphite shows a range of friction coefficient from 0.07 to 0.5 [1].

Soft metals are also being used as solid lubricants since they are soft in nature which provide maximum contact area when rubbing against harder surface for load support. Furthermore, soft metals can imbed abrasive debris and neutralize it [2]. Wear debris is often made harder by oxidation and work hardening which leads to poor surface interactions as a result of the three-body abrasive wear process [3]. Soft metals used

commercially as coating on strong metals where the coating provides self-lubricity while the substrate supports the normal load. Thin coatings tend to wear out quickly and thick coatings may reveal adherent issues or cause excessive deformation [2]. In their pure state, soft metals show low mechanical properties such as compressive and tensile strengths. In addition, their hardness values are in the range of 25 – 50 HV [2]. That makes them less attractive for structural applications and limits their use as coating materials. Another drawback is related to their melting point; some soft metals like tin, lead, indium and bismuth have melting points below 340 °C which cause metals to soften and oxidized at generally low temperatures [1].

Novel ternary nanolaminates, MAX phases, have been studied extensively over the last decade due their superior mechanical properties and tribological behaviors [4]. Some recent studies show excellent tribological behavior of MAX phases at elevated temperatures [4]. Also, it has been reported that adding such materials as the reinforcement phase in a matrix helped in improving mechanical and tribological properties [5-7].

## **1.2 MAX Phase**

MAX phases are layered, hexagonal carbides and nitrides with general formula  $M_{n+1}AX_n$ . (MAX) where  $n=1-3$ , M stands for the early transition metal, A stands for group-A elements and X are either carbon or nitrogen. Fig 1.1 shows the different combinations that can be used to fabricate MAX phases. MAX phases show unique and remarkable properties. MAX phases are highly damage tolerant, oxidation resistant, readily machinable and soft (2-8 GPa) [4, 8]. Moreover, MAX phases are excellent thermal and electrical conductors. By reviewing the previous properties, we can conclude that MAX

phases has the best properties of both metals and ceramics. It can be further classified as an intermediate class between metals and ceramics [9]. A comprehensive review has been done on MAX phases by Barsoum showed MAX phases incorporate both the properties of metal and ceramic in 2000 [8].

MAX phases consist of over 60 different ternary carbides and nitrides. When  $n=1, 2$  and 3 the series of MAX phases are known as 211, 312, 413 respectively [13]. The unit cell of MAX phases for 3 different series of MAX phases are shown in figure 1.2.

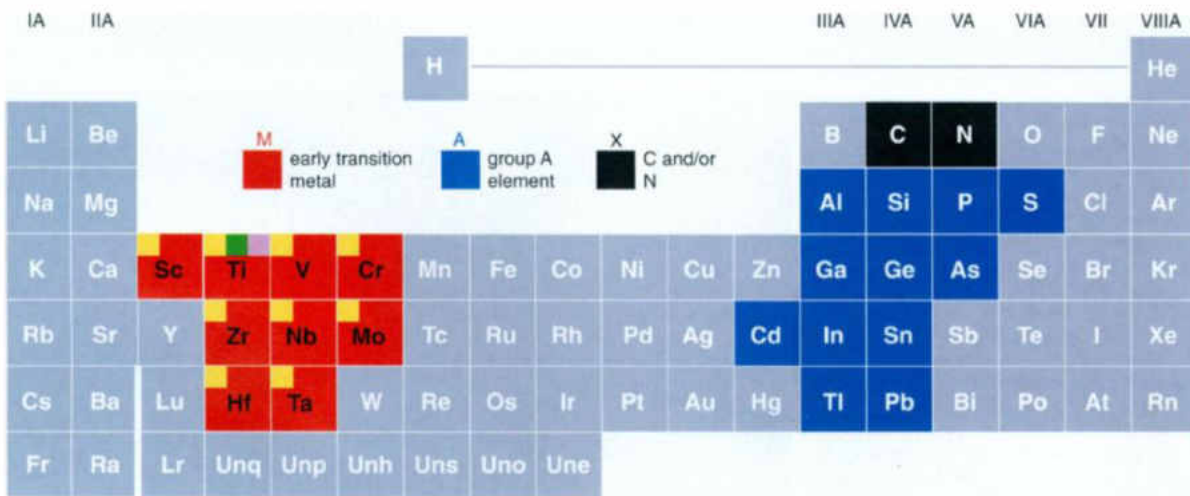


Fig 1.1 Possible combination of MAX phases [13]



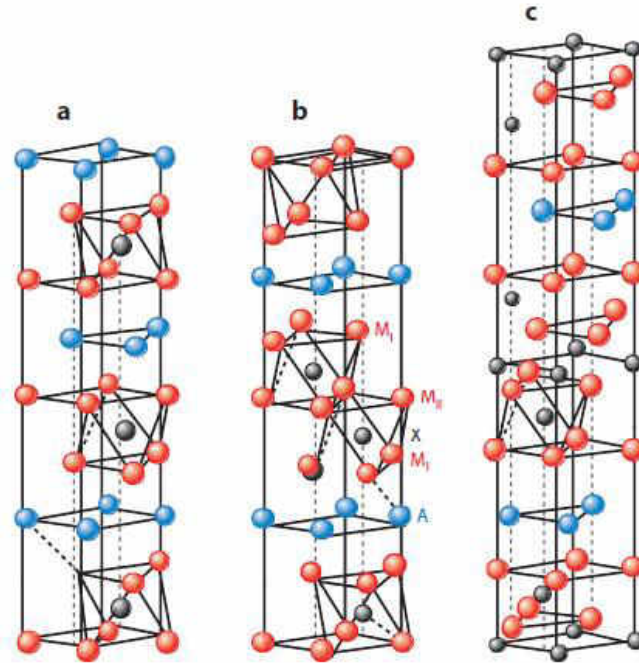


Fig 1.2 Unit Cell for 211(a), 312 (b) and 413 (c) series of MAX phases [13]

The layered structure of MAX phases and their high machinability in dry conditions indicate that they might show solid lubricity [9]. For example, Sarkar et al. [10] studied the tribology of  $Ti_3SiC_2$  against steel using a ball-on-disc method under fretting condition as the load was varied between 1 and 10 N. The  $\mu$ 's they obtained varied between 0.5-0.6, and the WRs were between  $(11-37) \times 10^{-5} \text{ mm}^3/\text{N.m}$ . Moreover, Gupta [11] studied tribological behavior of numerous MAX phases which include  $Ti_3SiC_2$  and  $Cr_2AlC$  at RT and 550 °C. His study concluded that MAX phases perform better at higher temperatures where wear rates were negligible and accompanied by friction coefficient of less than 0.5.

### 1.3 Introduction of MAX Reinforced Metals (MRMs)

MAX reinforced metals (MRMs) are the composites made from metal matrix where MAX phase is used as particulate reinforcement. Gupta et al. [4] showed that MAX phases at room temperature shows dual characteristics; in stage one they show low friction coefficient and wear but in stage two they show high friction coefficient and wear. That is mainly because of the formation of third body abrasion in the later stage. But at high-temperature MAX phases shows low friction coefficient and negligible wear [4, 11]. Summary of his work at room temperature is shown in Figure 1.3. Also, Gupta et al. [12] showed that MAX phase can be used as a particulate reinforcement to the polymer matrix. When composites are made of polymer matrix and MAX phases are used as a particulate reinforcement it is called MAX reinforced polymers (MRP) [12]. The study revealed that the addition of  $Ti_3SiC_2$  improved the mechanical and tribological properties of the polymer matrix. For example, the compressive strength and hardness were increased greatly as the concentration of the MAX phase increased. In addition, friction coefficient and wear rates decreased significantly as compared to the pristine epoxy.

There are earlier studies on the MAX reinforced metals (MRMs) composites by Gupta et al. [5-7]. In these studies,  $Ti_3SiC_2$  was used as reinforcement phase in aluminum (Al), tin (Sn) and zinc (Zn). Gupta et al. showed that the addition of hard, machinable and lubricious MAX phase particles to metals can impart self-lubricity and improve the mechanical and tribological behavior of metal matrix composites.

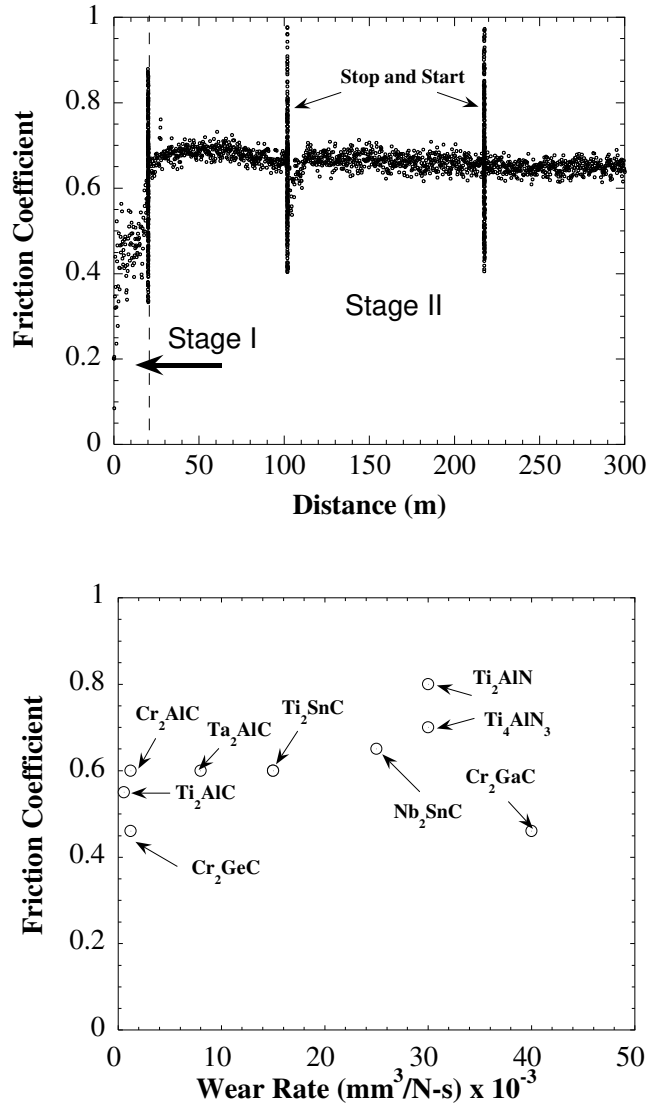


Fig. 1.3 Tribological performance of MAX phases at room temperature [11]

As shown in Figure 1.4, the compressive strength of Sn- $\text{Ti}_3\text{SiC}_2$  composites were increased gradually from 47 MPa for pure Sn to 75 MPa for the 30% concentration of  $\text{Ti}_3\text{SiC}_2$ . The same trend was also observed in Al- $\text{Ti}_3\text{SiC}_2$  where compressive strength increased significantly as  $\text{Ti}_3\text{SiC}_2$  content increased in the composition. However, at higher concentrations, 35 vol%, the strength decreased sharply. The authors suggest that the high porosity, ~ 25% porosity, of the sample degrades the strength of the composition. On contrary, the addition of  $\text{Ti}_3\text{SiC}_2$  did not improve nor deteriorate the compressive

strength significantly of the Zn-Ti<sub>3</sub>SiC<sub>2</sub> composites. Compressive strength values changed slightly from the pure Zn. The authors emphasize that the mechanical performance of the MRM is influenced by the ductility of the metal matrix, processing parameters, and interaction of Ti<sub>3</sub>SiC<sub>2</sub> particulates with metal matrix [7]. For example, it is well known that hexagonal metals like Zn are less ductile compared to Al.

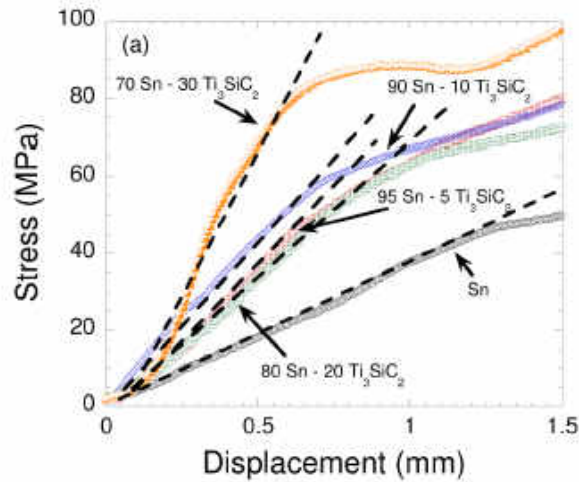


Fig 1.4 Compressive Strength of Sn-Ti<sub>3</sub>SiC<sub>2</sub> composites [6]

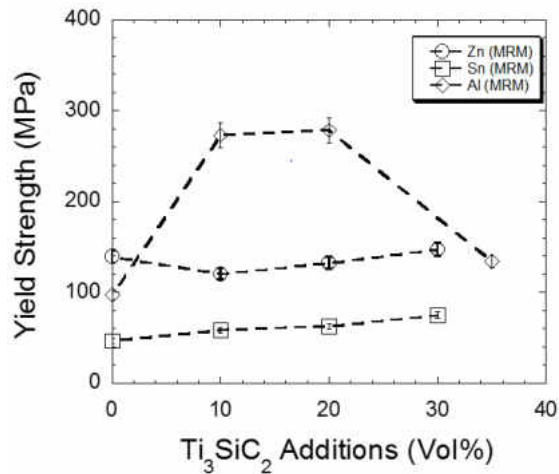


Fig 1.5 Summary of Compressive Strength of different MRM composites [5-7]

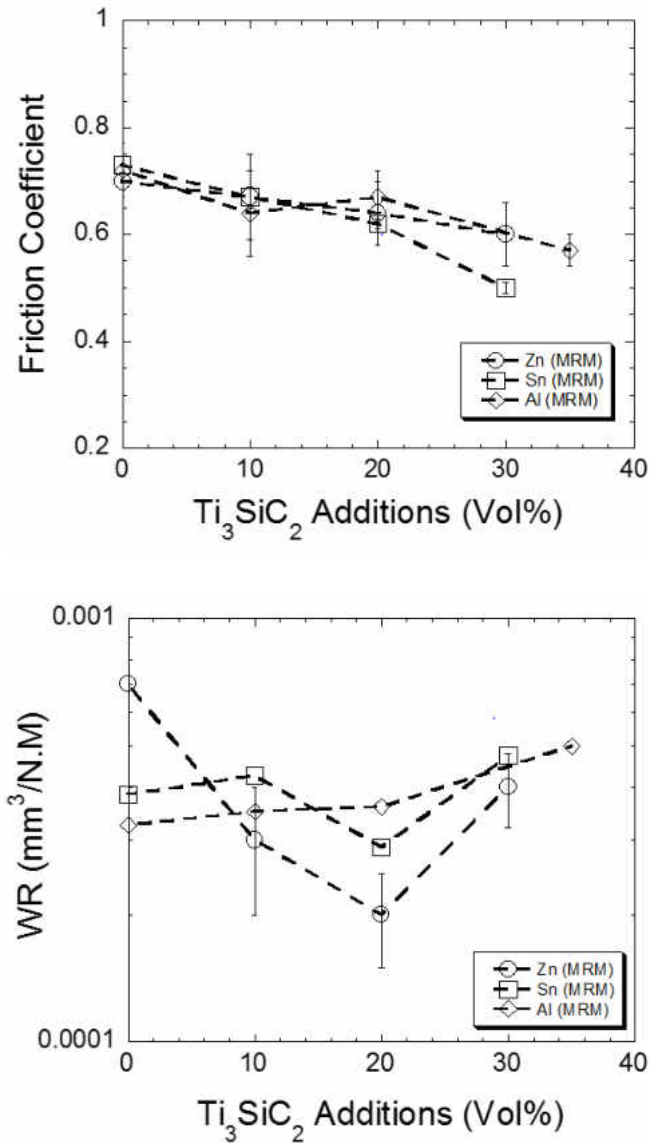


Fig 1.6. Tribological performances of different MRM composite [5-7]

Figure 1.6 shows tribological performance of Zn- $Ti_3SiC_2$ , Sn- $Ti_3SiC_2$  and Al- $Ti_3SiC_2$  composites. It is evident that the addition of  $Ti_3SiC_2$  directly impacted the friction coefficient of the MRM composite and resulted in low friction coefficient comparing with the pure matrix. It has also noted that the addition of  $Ti_3SiC_2$  helped in stabilizing the friction coefficient and eliminating the huge fluctuation of the pure samples. On the other hand, wear rate (WR) of Sn- $Ti_3SiC_2$  composites were similar, and varied between (3-5) X

$10^{-4}$  mm<sup>3</sup>/N.m. However, the addition of 30 vol% of Ti<sub>3</sub>SiC<sub>2</sub> increased the WR to  $6 \times 10^{-4}$  mm<sup>3</sup>/N.m but it's accompanied with low friction coefficient ( $\mu \sim 0.4$ ). The WRs of Zn-Ti<sub>3</sub>SiC<sub>2</sub> composites varied between in the range of  $(2-7) \times 10^{-4}$  mm<sup>3</sup>/N.m. The addition of Ti<sub>3</sub>SiC<sub>2</sub> particulates marginally decreased the WRs compared to the pure Zn, and showed an optimum value of  $2 \times 10^{-4}$  mm<sup>3</sup>/N.m for the addition of 20 vol% of Ti<sub>3</sub>SiC<sub>2</sub>. The higher WR of increasing Ti<sub>3</sub>SiC<sub>2</sub> content to 30 vol% can be due to the brittle nature of these composites. For Al-Ti<sub>3</sub>SiC<sub>2</sub> composites, the WRs were in the range of  $(2-5) \times 10^{-4}$  mm<sup>3</sup>/N.m and accompanied by lower friction coefficients comparing with the pure Al. It's well established now that there are beneficial effects on the mechanical and tribological properties of soft metals because of adding Ti<sub>3</sub>SiC<sub>2</sub> to the matrix. However, the performance of MRM composites is influenced by the ductility of the metal matrix, processing parameters, and interaction of Ti<sub>3</sub>SiC<sub>2</sub> particulates with metal matrix [7].

#### **1.4 Current Research Effort**

During this thesis, different soft metals (Ag, Bi & Al) were selected as the main constituents for the composite “matrix” and reinforced with different MAX phases (Ti<sub>3</sub>SiC<sub>2</sub>, Cr<sub>2</sub>AlC & V<sub>2</sub>AlC) as reinforcement phase. The MAX phase will enhance the mechanical performance of MRM composites by increasing the compressive strength and hardness. In addition, MAX phase will have beneficial effect on the tribological behavior of MRM composites by decreasing the friction coefficient and the wear rate. Synthesis and characterization of Bi-Ti<sub>3</sub>SiC<sub>2</sub> and Ag-Ti<sub>3</sub>SiC<sub>2</sub> will be studied in Chapter 2. Thereafter, Bi-Cr<sub>2</sub>AlC composites will be studied in Chapter 3 and the results will be compared to Bi-Ti<sub>3</sub>SiC<sub>2</sub> composites. In Chapter 4, the effect of adding Ti<sub>3</sub>SiC<sub>2</sub>, Cr<sub>2</sub>AlC and V<sub>2</sub>AlC to Al matrix will studied for their mechanical performance and tribological behavior.

## CHAPTER II

### Synthesis and Tribological Behavior of Novel Ag and Bi based MRMs (MAX Reinforced Metals)

**Abstract (Please note the content of this chapter has been accepted for publication in Wear):**

This work reports the synthesis and characterization of Bi-Ti<sub>3</sub>SiC<sub>2</sub> and Ag-Ti<sub>3</sub>SiC<sub>2</sub> composites for the first time. The addition of Ti<sub>3</sub>SiC<sub>2</sub> particulates enhanced the hardness and compressive yield strength of both the compositions. Bi-based MRM systems showed an enhancement in yield strength from ~42 MPa in Bi to ~71 MPa in Bi-30 Vol% Ti<sub>3</sub>SiC<sub>2</sub> (enhancement in strength by ~1.7 times). Similarly, Ag-based MRM systems showed an enhancement from ~47 MPa in Ag to ~164 MPa in Ag-20 Vol% Ti<sub>3</sub>SiC<sub>2</sub> (enhancement in strength by ~3.5 times). The addition of Ti<sub>3</sub>SiC<sub>2</sub> particulates also had a remarkable effect on tribological performance. All the samples were tested by block (tab)-on-disk method. The  $\mu_{\text{mean}}$  decreased gradually from ~0.38 in Ag to ~0.30 in Ag-30 Vol% Ti<sub>3</sub>SiC<sub>2</sub>. Similarly, the  $\mu_{\text{mean}}$  decreased gradually from ~0.50 in Bi to ~0.41 in Bi-20 Vol% Ti<sub>3</sub>SiC<sub>2</sub>, thereafter it increased ~0.53 in Bi-70%312Si. The WR of Ag decreased from  $4.9 \times 10^{-5}$  mm<sup>3</sup>/N.m to  $4.2 \times 10^{-6}$  mm<sup>3</sup>/N.m in Ag-20 Vol% Ti<sub>3</sub>SiC<sub>2</sub> (decreased by ~12 times). Similarly, Bi had a WR of 0.02 mm<sup>3</sup>/N.m, and it decreased to  $3 \times 10^{-4}$  mm<sup>3</sup>/N.m in Bi-10 Vol% Ti<sub>3</sub>SiC<sub>2</sub>, and marginally increased to  $6 \times 10^{-4}$  mm<sup>3</sup>/N.m and  $4.5 \times 10^{-4}$  mm<sup>3</sup>/N.m in Bi-20 Vol% Ti<sub>3</sub>SiC<sub>2</sub> and Bi-30 Vol% Ti<sub>3</sub>SiC<sub>2</sub>, respectively. In other words, the addition of 20 Vol% Ti<sub>3</sub>SiC<sub>2</sub> particulates decreased the WR by ~33 times. Detailed SEM studies showed that the tribological behavior is governed by the formation of Type IVa tribofilms. The presented work in this chapter has been accepted for publication in Wear journal.

## 2.1 Introduction

Soft metals like Ag, Bi, and their composites are promising materials for designing novel materials which possess enhanced mechanical properties along with functional properties like solid lubrication, tailored hardness, and corrosion resistance, among others. These materials can be potentially used in space-age transportation systems, air-foil bearings, biomedical applications, propulsion bearing and fasteners, thermal interface materials (TIMs), among others [1-12]. More particularly, different studies are being pursued to use Ag and their composites as solid lubricant materials for different applications over a wide range of temperatures [1-9]. Similarly, Bi can be considered as a green alternative to Pb and has been studied for solid lubrication and hot forming [10-12].

Gupta et al. [3] have shown that composites of MAX phases ( $\text{Cr}_2\text{AlC}$  and  $\text{Ta}_2\text{AlC}$ ) with Ag can be used as a solid lubricant over a wide range of temperatures. Wang et al. [20] have shown that Al-matrix material composites fabricated from pure Al and 40 vol%  $\text{Ti}_3\text{AlC}_2$  powders have twice the yield strength of pure aluminum. Hu et al. [21] have shown AA6061/ $\text{Ti}_2\text{AlC}$  composites had 1.5 times the specific yield strength of peak aged AA6061. Recently, Gupta et al. [24-26] showed that the addition of  $\text{Ti}_3\text{SiC}_2$  particulates enhanced the mechanical and tribological performance of Al-matrix, Sn-matrix, and Zn-matrix composites. In this work, we will report the effect of  $\text{Ti}_3\text{SiC}_2$  particulates on the mechanical and tribological behavior of Bi- and Ag- based MRM composites.



## 2.2 Experimental Methods

Ti<sub>3</sub>SiC<sub>2</sub> powder (-325 mesh, Kanthal, Hallstahammar, Sweden) and calculated concentrations of metal powders (Ag powders (5-8 μm, Sigma Aldrich, St. Louis, MO) or Bi powders (-100 mesh, Sigma Aldrich, St. Louis, MO)) were dry ball milled (8000 M mixer Mill, SPEX SamplePrep, Metuchen, NJ) for 2 minutes. All the powders were then poured in a die. Ag-based compositions were cold-pressed at ~232 MPa (the cycle was repeated twice) in a ~6.35 mm die (EQ-Die-06D, MTI Corporation, Richmond, CA), and sintered at 900 °C for 10 min. For comparison, samples of pure Ag were also fabricated by following the above mentioned method. Bi-based were difficult to machine as they were soft at low concentration of Ti<sub>3</sub>SiC<sub>2</sub> or brittle at 30 vol% Ti<sub>3</sub>SiC<sub>2</sub>, thus, in order to minimize machining, two sets of Bi-based compositions were fabricated by using ~12.7 mm (EQ-Die-12D-B, MTI Corporation, Richmond, CA) and ~6.35 mm (EQ-Die-06D, MTI Corporation, Richmond, CA), respectively. The Bi-based compositions were then sintered in atmospheric air by hot pressing (HP) with a uniaxial compressive stress of ~201 MPa (~12.7 mm die) or ~251 MPa (~6.35 mm) at 290 °C for 5 minutes. Samples from the former set were used for tribology and hardness studies where samples from the latter set were used for mechanical performance. Composites were allowed to cool in the HP to room temperature (RT) before characterization. For comparison, samples of pure Bi were also fabricated by following the above mentioned method. Ag-based MRM composites were designed by adding 30 vol% (Ag-30 vol% Ti<sub>3</sub>SiC<sub>2</sub>), 20 vol% (Ag-20 vol% Ti<sub>3</sub>SiC<sub>2</sub>), 10 vol% (Ag-10 vol% Ti<sub>3</sub>SiC<sub>2</sub>), 5 vol% (Ag-5 vol% Ti<sub>3</sub>SiC<sub>2</sub>) Ti<sub>3</sub>SiC<sub>2</sub> in the Ag matrix. Similarly, Bi-based MRM composites were designed by 30 vol% (Bi-30 vol%

Ti<sub>3</sub>SiC<sub>2</sub>) 20 vol% (Bi-20 vol% Ti<sub>3</sub>SiC<sub>2</sub>), 10 vol% (Bi-30 vol% Ti<sub>3</sub>SiC<sub>2</sub>), 5 vol% (Bi-5 vol% Ti<sub>3</sub>SiC<sub>2</sub>) Ti<sub>3</sub>SiC<sub>2</sub> in the Bi- matrix.

Rule of mixtures was used to calculate the theoretical density of all the composite samples by using the theoretical density of Ti<sub>3</sub>SiC<sub>2</sub> and metal particulates. The experimental density of the composites was then calculated from the mass and dimensions of each sample. The relative density (RD) was then calculated by normalizing the experimental density with theoretical density. Thereafter the porosity is calculated from:

$$\text{Porosity}\% = (1 - \text{RD}) \times 100$$

Samples of Ag-based compositions and Bi-based compositions were mildly polished and were then used directly after HP for mechanical testing. These samples were then tested in a mechanical testing unit in compression (Shimadzu AD-IS UTM, Shimadzu Scientific Instruments Inc., Columbia, MD). For each composition, a set of 3 samples were tested at a deflection rate of 1 mm/min. Stress versus displacement plots are reported as experimental limitations did not allow for accurate measurement of the actual strain during mechanical testing. In this work, yield strength is defined as the critical stress at which the stress versus displacement plot transitions from the linear to nonlinear regime. The linear region of the composites had a regression fitting of  $R^2 > 0.95$ . Reported within this text is the average of 3 yield strength measurements for each composite [24-26]. All composites were polished ( $R_a < 1 \mu\text{m}$ ) and then tested by a Vicker's micro-hardness indenter (Mitutoyo HM-112, Mitutoyo Corporation, Aurora, IL). For Ag-based MRMs, Vicker's hardness was performed by loading the samples at 4.9 N for 12 s, and Bi-based MRMs were tested by loading the samples at 0.49 N for 12 s. In this research, an average of five readings for each composite system is reported.

XRD measurements were performed by a Rigaku Diffractometer (SmartLab, Rigaku, Japan) at a scan rate of  $0.05^\circ$  /min from  $20^\circ$  to  $70^\circ$ . The tribological behavior of the samples were tested by using a block (tab)-on-disc tribometer (CSM Instruments SA, Peseux, Switzerland) at 5 N ( $\sim 0.3$  MPa), 50 cm/s linear speed, 1000 m sliding distance, and  $\sim 10$  mm track radius against alumina disks (AL-D-42-2, AdValue Technology, Tucson, AZ). Pure Bi samples were tested for only  $\sim 80$  m as they had a higher wear. For tribological testing, the blocks were machined in the dimensions of  $\sim 4$  mm x  $\sim 4$  mm x  $\sim 3$  mm samples, and then they were polished to a  $\sim 1$   $\mu$ m finish. Alumina disks were also polished to a  $\sim 1$   $\mu$ m finish. A surface profilometer (Surfcom 480A, Tokyo Seimitsu Co. Ltd., Japan) was used to confirm that all the samples had a  $R_a < 1$   $\mu$ m. For each composition, three experimental studies for tribological studies were performed. For data analysis, an average of all the friction coefficients ( $\mu$ ) reading was used to calculate mean response of a single experiment. Thereafter, average of three means was calculated and reported in the text as  $\mu_{\text{mean}}$ . The mass of the samples and substrates were measured before and after the testing using a scale (Model AL204, Mettler Toledo, Columbus, OH). The specific wear rate (WR) was calculated from:

$$WR = (m_i - m_f) / (\rho \cdot N \cdot d)$$

where,  $m_i$  is the initial mass,  $m_f$  is the final mass,  $\rho$  is density of the composite,  $N$  is the applied load, and  $d$  is the total distance traversed by the tab during the tribology testing [24-26].

Alumina samples were coated with Au/Pd by using a Balzers SCD 030 sputter coater (BAL-TEC RMC, Tucson AZ USA), and then mounted on aluminum mounts. For all samples, secondary electron (SE) and backscattered electrons (BSE) images were

obtained by using a JEOL JSM-6490LV Scanning Electron Microscope (JEOL USA, Inc., Peabody, Massachusetts.) X-ray information was obtained via a Thermo NanoTrace Energy Dispersive Xray detector with NSS-300e acquisition engine. It is critical to note that the accuracy of measuring the presence of carbon is quite low in the EDS. Thus, it is expected that all the compositions listed, especially sub-stoichiometric oxides, could very well contain C. In the text, \*microconstituent\* is defined as the region where the chemistry of a region is deemed chemically uniform at the micron level as quantified by Energy Dispersive Spectroscopy (EDS). It will be designated with two asterisks, as to emphasize that these areas are not necessarily single phases, and the presence of C in these tribofilms will be shown by adding {C<sub>x</sub>} in the composition [2]. For comparing grain size, Bi and Bi-20 vol% Ti<sub>3</sub>SiC<sub>2</sub> samples were etched using H<sub>2</sub>O (distilled water (DI water)) and HCl (ACS Reagent 37%, Sigma Aldrich, St. Louis, MO)) mixed in the ratio of 10:1. Ag and Ag-20 vol% Ti<sub>3</sub>SiC<sub>2</sub> samples were etched using H<sub>2</sub>O, HCl, and HNO<sub>3</sub> (ACS Reagent 70%, Sigma Aldrich, St. Louis, MO)) in the ratio of 2.2:1.0:1.05. All the polished samples were etched for ~30 s and then cleansed with DI water. The etched samples were inspected by a Scanning Electron Microscope (650 FEG, FEI Company, Hillsboro, OR). The length of each individual grain was measured by Image J software. An average of 100 grains is reported for each sample. Image J software is a Java-based public domain software [27].

## **2.3 Results and Discussion**

### **2.3.1 Microstructure and Phase Analysis**

Figures 2.1 – 2.2 show SE images of different Bi-, and Ag-based MRM composites. In all the compositions, the Ti<sub>3</sub>SiC<sub>2</sub> particulates are well-dispersed in the metal matrix. As an illustration, Fig. 2.1d shows a Ti<sub>3</sub>SiC<sub>2</sub> particulate embedded in the Bi-10 vol% Ti<sub>3</sub>SiC<sub>2</sub> matrix with negligible interfacial reaction. Similarly, Fig. 2.2d shows Ti<sub>3</sub>SiC<sub>2</sub> particle inside

the Ag-10 vol%  $\text{Ti}_3\text{SiC}_2$  matrix with no signs of interfacial reaction. Figures 2.3a-b show the etched surfaces of Bi and Bi-20 vol%  $\text{Ti}_3\text{SiC}_2$ . Both the samples had similar micron-sized grains of  $(18.67 \pm 8.88) \mu\text{m}$  and  $(23.62 \pm 8.17) \mu\text{m}$ , respectively. Similarly, Figures 2.3c-d show the etched surfaces of Ag and Ag-20 vol%  $\text{Ti}_3\text{SiC}_2$ , and the grain size of both the samples were  $(0.399 \pm 0.097) \mu\text{m}$  and  $(0.533 \pm 0.278) \mu\text{m}$ , respectively. The addition of  $\text{Ti}_3\text{SiC}_2$  particulates do not have a drastic effect on the grain size. Figure 2.4 shows the XRD plots of all the designed MRM composites. By analyzing the XRD diffraction and SEM micrographs - it can be concluded that there is minimal reaction between the metal and  $\text{Ti}_3\text{SiC}_2$  particulates.

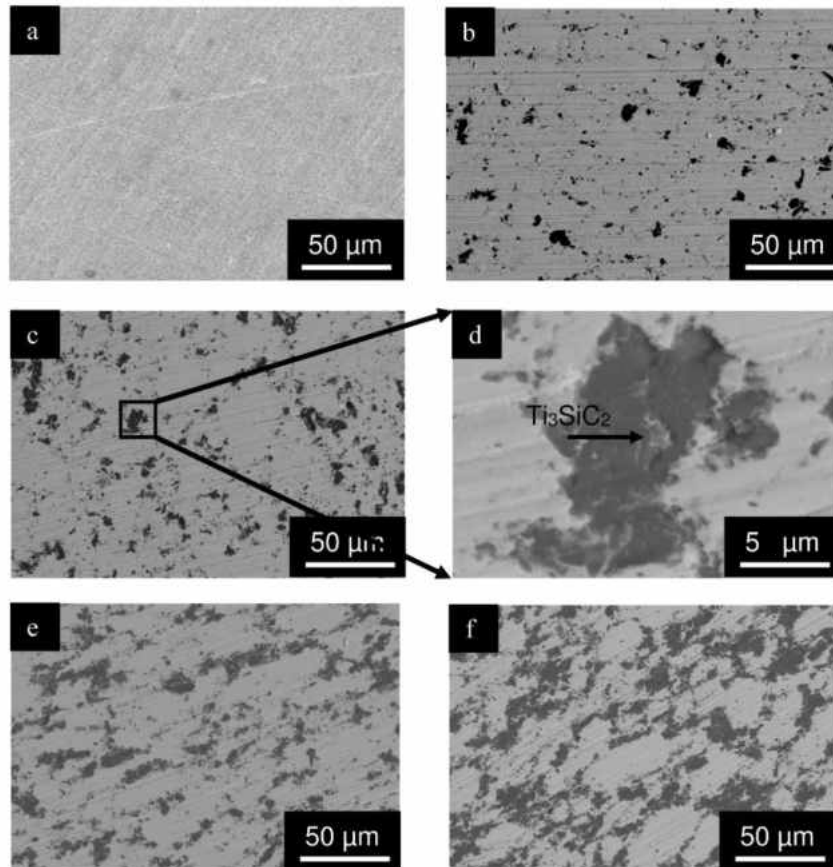


Fig 2.1 SEM of (a) Bi in SE, (b) Bi-5 vol%  $\text{Ti}_3\text{SiC}_2$ , (c) Bi-10 vol%  $\text{Ti}_3\text{SiC}_2$ , (d) higher magnification of the marked region in (c), (e) Bi-20 vol%  $\text{Ti}_3\text{SiC}_2$ , and (f) Bi-30 vol%  $\text{Ti}_3\text{SiC}_2$  in BSE.

Figure 2.6a shows porosity of the composites as a function of  $\text{Ti}_3\text{SiC}_2$  additions. In all Bi-based MRM samples, porosity increased with the addition of higher vol% of  $\text{Ti}_3\text{SiC}_2$  concentrations which indicates that it becomes difficult to process these samples as the amount of  $\text{Ti}_3\text{SiC}_2$  is increased in the metal matrix. A similar trend was also observed during the processing of Al- [24], Sn- [25], and Zn- [26] based MRM composites.

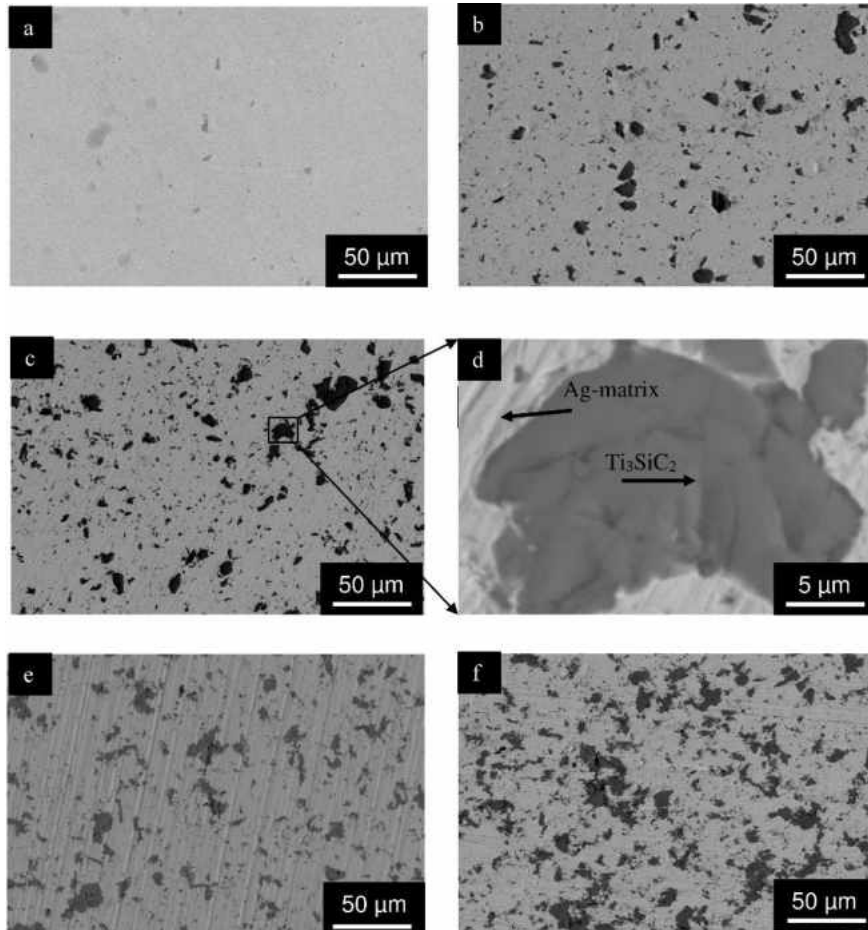


Fig 2.2 SEM BSE images of (a) Ag, (b) Ag-5 vol%  $\text{Ti}_3\text{SiC}_2$ , (c) Ag-10 vol%  $\text{Ti}_3\text{SiC}_2$ , (d) higher magnification of the marked region in (c), (e) Ag-20 vol%  $\text{Ti}_3\text{SiC}_2$ , and (f) Ag-30 vol%  $\text{Ti}_3\text{SiC}_2$ .

Interestingly, the porosity of the Ag-based MRMs decreased from ~39% in Ag to ~13% in Ag-5 vol%  $\text{Ti}_3\text{SiC}_2$ , thereafter it increased marginally to ~18% in Ag-10 vol%  $\text{Ti}_3\text{SiC}_2$ , and retained similar values at higher concentration of  $\text{Ti}_3\text{SiC}_2$  additions (Fig. 2.5a). This important result shows that  $\text{Ti}_3\text{SiC}_2$  can be used as sintering additives for

sintering Ag and its composites during pressureless sintering. As a comparison, Panigrahi et al. [28] have shown that metallic addition like 1 wt% Ni can enhance the sintering of  $Ti_3SiC_2$  but no studies have been performed to study the effect of  $Ti_3SiC_2$  particulates on the sintering of metallic systems. This study shows that  $Ti_3SiC_2$  particulates can be an effective sintering aid for Ag-based system and warrants further fundamental research to understand the exact mechanism.

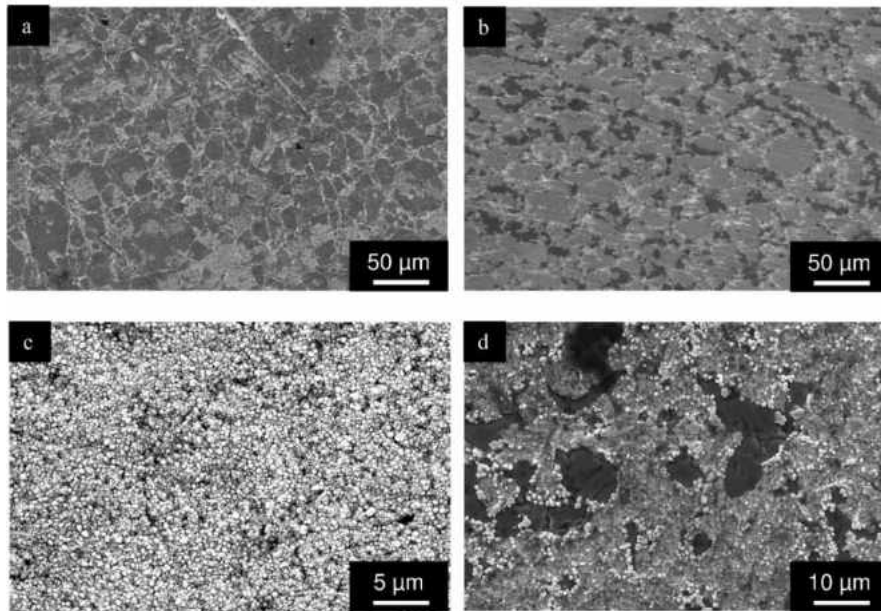


Fig 2.3 SE SEM micrographs of etched surfaces of (a) Bi, (b) Bi-20 vol%  $Ti_3SiC_2$ , (c) Ag, and (d) Ag-20 vol%  $Ti_3SiC_2$ .

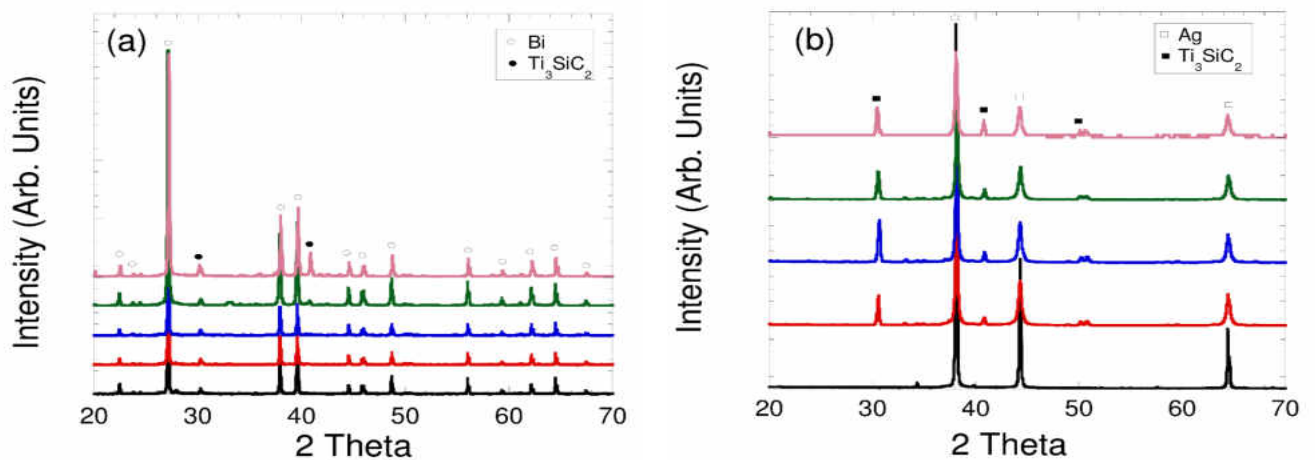


Fig 2.4 Plot of XRD patterns of, (a) Bi-based MRMs, and (b) Ag-based MRMs.

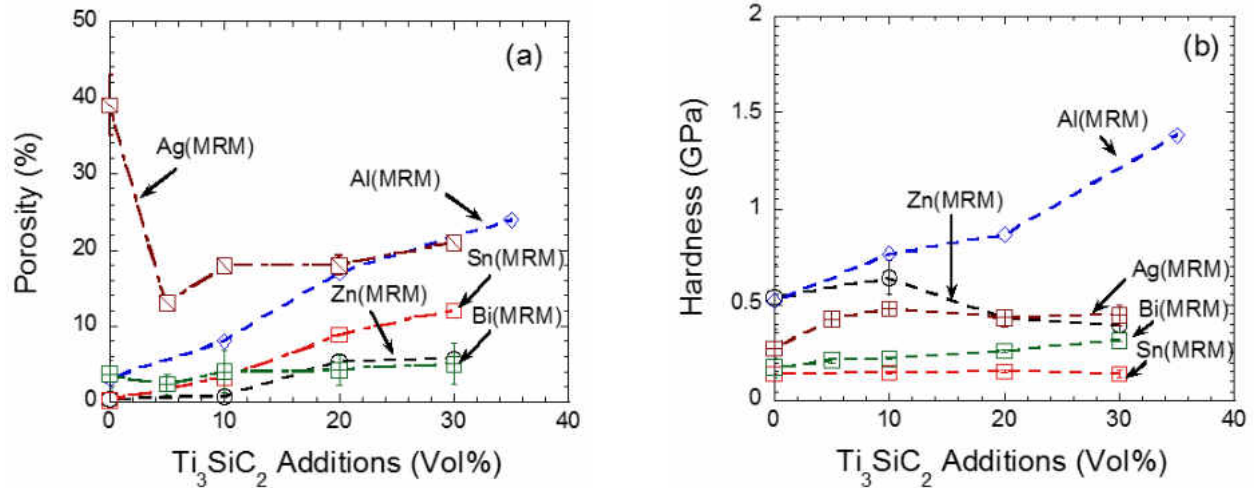


Fig 2.5 Plots of variation of (a) porosity, and (b) hardness versus  $Ti_3SiC_2$  additions.

Figure 2.5b plots the variation of hardness as a function of  $Ti_3SiC_2$  content. In Bi-based MRMs, the hardness increased gradually from  $\sim 0.17$  GPa in Bi to  $\sim 0.31$  GPa in Bi-30 vol%  $Ti_3SiC_2$ . Similarly, in Ag-based MRMs the hardness increased from  $\sim 0.27$  GPa to  $\sim 0.48$  GPa in Ag-10 vol%  $Ti_3SiC_2$ , thereafter, it decreased marginally to  $\sim 0.43$  GPa and  $\sim 0.45$  GPa in Ag-20 vol%  $Ti_3SiC_2$  and Ag-30 vol%  $Ti_3SiC_2$ , respectively. In general, the addition of hard  $Ti_3SiC_2$  particulates increased the hardness of the composites, but the presence of porosity in samples Sn accounts for the slight decreased in hardness of Ag-20 vol%  $Ti_3SiC_2$  and Ag-30 vol%  $Ti_3SiC_2$  as compared to Ag-10 vol%  $Ti_3SiC_2$ . A similar trend was also observed in Al- [24], Sn- [25], and Zn- [26] based MRM composites.

### 2.3.2 Mechanical Performance of MRMs

Figures 2.6a-b plot the compressive strength versus displacement of Bi-based and Ag-based MRMs, respectively. Brittle failure is observed in Bi-30 vol%  $Ti_3SiC_2$  (Fig. 2.6a) and Ag-30 vol%  $Ti_3SiC_2$  (Fig. 2.6b) whereas all the other compositions showed gradual failure. However, in general, the compressive yield strength is improved as the concentration of  $Ti_3SiC_2$  particulates is increased in the matrix (Fig. 2.6c). For example,



for Bi-based MRMs; the yield strength improved from ~42 MPa in Bi to ~71 MPa in Bi-30 vol%  $Ti_3SiC_2$  (an enhancement of 1.7 times as compared to pristine Bi).

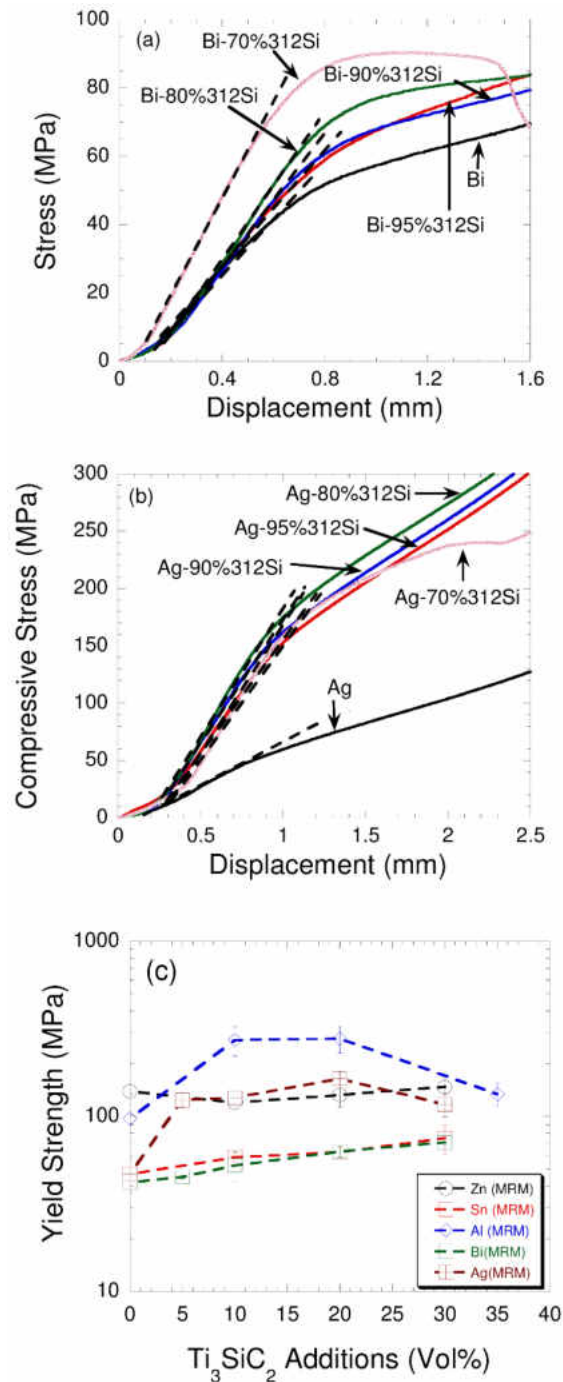


Fig 2.6 Plot of (a) stress versus displacement of Bi MRMs, (b) stress versus displacement Ag MRMs, and (c) yield strength of different MRMs versus  $Ti_3SiC_2$  additions [24-26].

For Ag-based MRMs, the yield strength improved from ~47 MPa in Ag to ~164 MPa in Ag-20 vol%  $\text{Ti}_3\text{SiC}_2$  (an enhancement of 3.5 times as compared to pristine Ag); thereafter, it dropped to ~117 MPa in Ag-30 vol%  $\text{Ti}_3\text{SiC}_2$ . The brittle failure in Ag-30 vol%  $\text{Ti}_3\text{SiC}_2$  can account for the decrease in yield strength as compared to Ag-30 vol%  $\text{Ti}_3\text{SiC}_2$ . Comparatively, Al-and Sn-based MRMs showed similar behavior, but Zn-based MRMs did not show any enhancement in yield strength [24-26] (Fig. 2.6c). By analyzing these results, it can be concluded that mechanical performance of the MRMs is affected by a host of factors like ductility of the base metal, processing parameters, and subtle interactions of  $\text{Ti}_3\text{SiC}_2$  particulates with the metal matrix which can affect dislocation motion, and sintering and grain growth kinetics.

### 2.3.3 Tribological Behavior of MRMs

Figure 2.7 shows the plot of  $\mu$  versus distance profile of Bi- (Fig. 2.7a), and Ag- (Fig. 2.7b) based MRMs. In all the cases, it can be easily construed that the addition of  $\text{Ti}_3\text{SiC}_2$  particulates have a direct impact on the  $\mu$  of the MRMs. For example, Bi had a very high  $\mu$  (~0.7) after cycling for ~80 m as compared to Bi-based MRM which were cycled for 1000 m (Fig. 2.7 a). In these MRMs, initially, the  $\mu$  was low (Region I), but it gradually reached steady state (Region II). Similarly, Ag showed erratic behavior as compared to Ag-based MRMs which showed initially a run-in period for ~200 m (region I), thereafter, it attained a steady state (Region II) (Fig. 2.7 b).

Figure 2.8 a compares the  $\mu_{\text{mean}}$  of all the MRMs. Ag-based MRMs have the lowest  $\mu_{\text{mean}}$  amongst all the compositions followed by Bi-based MRMs. More particularly, the  $\mu_{\text{mean}}$  decreased gradually from ~0.38 in Ag to ~0.30 in Ag-30 vol%  $\text{Ti}_3\text{SiC}_2$ . Similarly, the  $\mu_{\text{mean}}$  decreased gradually from ~0.50 in Bi to ~0.41 in Bi-20 vol%  $\text{Ti}_3\text{SiC}_2$ , thereafter it

increased  $\sim 0.53$  in Bi-30 vol%  $\text{Ti}_3\text{SiC}_2$ . Comparatively, Sn-, Zn-, and Al-based MRMs had higher  $\mu_{\text{mean}}$  as compared to Ag- and Bi-based MRMs but showed a decrease in  $\mu_{\text{mean}}$  as the concentration of  $\text{Ti}_3\text{SiC}_2$  particulates was increased in the metal matrix [24-26].

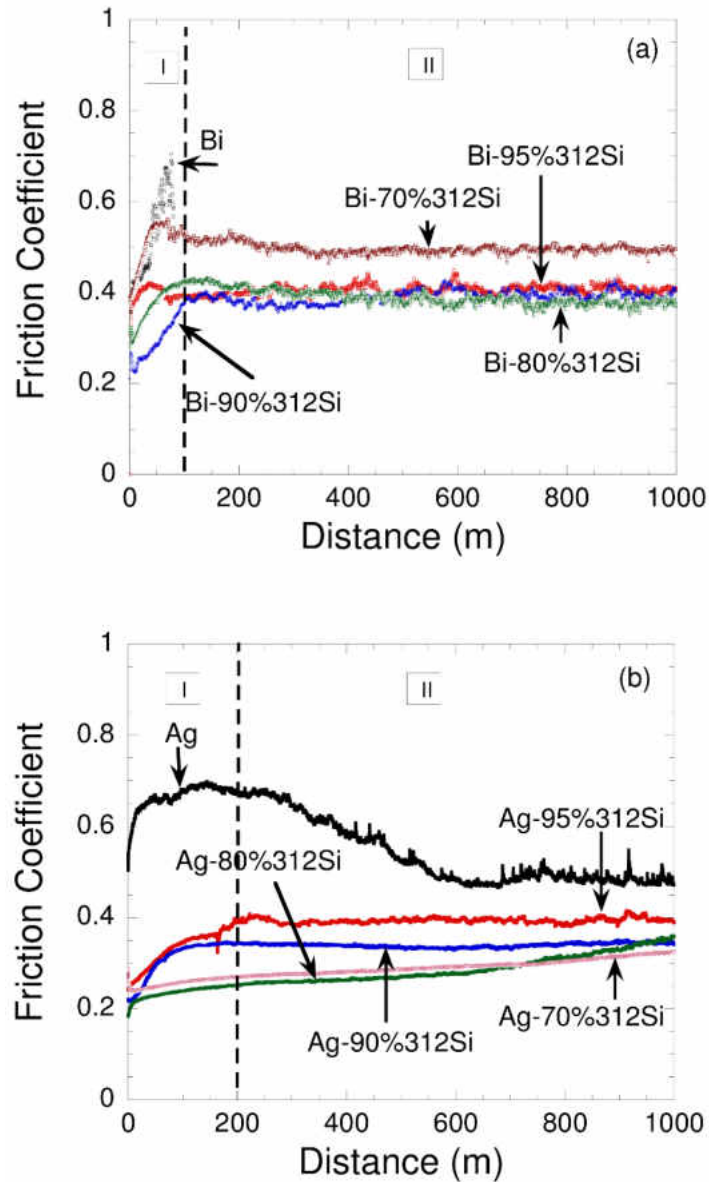


Fig 2.7 Plot of friction coefficient ( $\mu$ ) versus distance of (a) Bi-based MRMs, and (b) Ag-based MRMs.

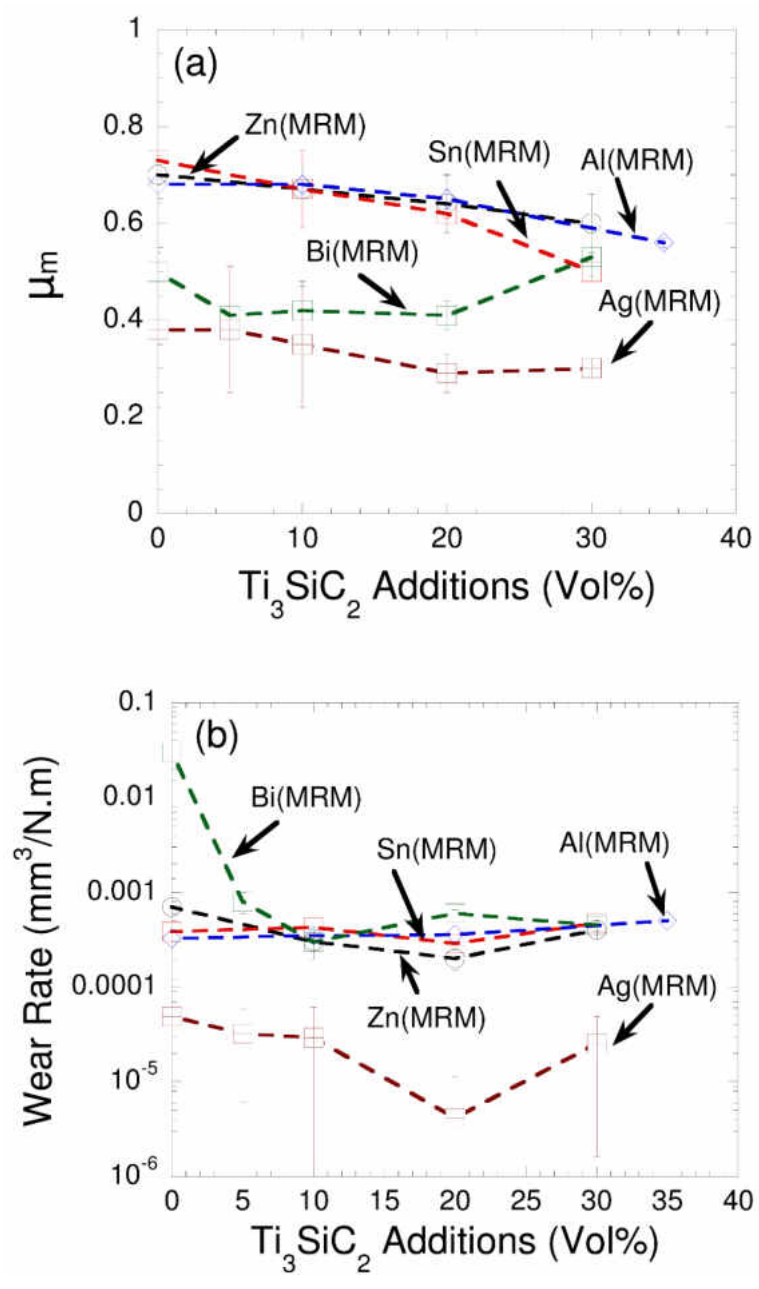


Fig 2.8 Plot of (a)  $\mu_{mean}$ , and (b) WR as a function of  $Ti_3SiC_2$  content for different MRMs [24-26].

Figure 2.8b plots the WRs of all MRMs. Ag-based MRMs showed the lowest WR. WR of Ag decreased gradually from  $4.9 \times 10^{-5} \text{ mm}^3/\text{N.m}$  to  $4.2 \times 10^{-6} \text{ mm}^3/\text{N.m}$  in Ag-20 vol%  $\text{Ti}_3\text{SiC}_2$ , and then increased to  $2.5 \times 10^{-5} \text{ mm}^3/\text{N.m}$  in Ag-70 vol%  $\text{Ti}_3\text{SiC}_2$ . In other words, the addition of 20 vol%  $\text{Ti}_3\text{SiC}_2$  decreased the WR by ~12 times. In literature, there are no results to compare these results with  $\text{Ti}_3\text{SiC}_2$ -Ag composites with greater >70 vol%  $\text{Ti}_3\text{SiC}_2$  content. In addition, it is very difficult to compare tribology results as they are done under different conditions according to the specific requirements of an application. For illustrative purposes, Table 2.1 compares tribological behavior of different Ag-based composites. Comparatively, composites of  $\text{Ta}_2\text{AlC}$  (TaAg11) and  $\text{Cr}_2\text{AlC}$  (CrAg11) with 20 vol% Ag showed a WR of  $\sim 3 \times 10^{-5} \text{ mm}^3/\text{N.m}$  and  $\sim 1 \times 10^{-4} \text{ mm}^3/\text{N.m}$ , respectively, during testing against alumina at 3 N load and 100 cm/s linear speed [3]. These results show that the addition 5-20 vol%  $\text{Ti}_3\text{SiC}_2$  can decrease the WR of Ag. In addition, among all the reviewed systems, Ag-MRMs and alumina tribocouples showed better or comparable results as other Ag-based tribocouples (Table 2.1). Li et al. [5] had outlined that two major drawbacks of using Ag-based lubricants: (a) limited life and replenishment of the solid lubricant, and (b) serious plastic deformation at higher temperatures. This work shows that Ag-based MRMs can be potential candidates for structural components due to their superior yield strength and enhanced tribological performance. In other words, Ag-based MRMs can be potential candidates for triboactive structural components. These exciting results also open new avenues for more fundamental research for high temperature solid lubrication studies.

Similarly, in Bi-based MRMs, Bi had a WR of  $\sim 0.02 \text{ mm}^3/\text{N.m}$ , and it decreased gradually to  $\sim 3 \times 10^{-4} \text{ mm}^3/\text{N.m}$  in Bi-10 vol%  $\text{Ti}_3\text{SiC}_2$ , and marginally increased to  $\sim 6 \times$

$10^{-4}$  mm<sup>3</sup>/N.m and  $4.5 \times 10^{-4}$  mm<sup>3</sup>/N.m in Bi-20 vol% Ti<sub>3</sub>SiC<sub>2</sub> and Bi-30 vol% Ti<sub>3</sub>SiC<sub>2</sub>, respectively. In other words, the addition of 10 and 20 vol% Ti<sub>3</sub>SiC<sub>2</sub> particulates decreased the WR by ~67 and ~33 times, respectively. As far as we are aware, this is the first study of the effect of Ti<sub>3</sub>SiC<sub>2</sub> particulates on the tribological behavior of Bi-based composites. Comparatively, the addition of Ti<sub>3</sub>SiC<sub>2</sub> particulates marginally decreased the WRs of Zn-based MRMs as compared to pure Zn metal and showed an optimum value of  $\sim 2 \times 10^{-4}$  mm<sup>3</sup>/N.m for Zn-20 vol% Ti<sub>3</sub>SiC<sub>2</sub> composite. The WRs of Al- and Sn-based MRMs were also in the same range (Fig. 2.8b). Based on these results, it can be concluded that Ti<sub>3</sub>SiC<sub>2</sub> particulates are excellent candidates as solid lubricants over a wide range of metallic systems.

Table 2.1: Comparison of tribological behavior of different Ag-based composites.

Composition	Countersurface	Conditions	WR (mm <sup>3</sup> /N.m)	Friction	Ref.
Ta <sub>2</sub> AlC - 20 vol% Ag	Alumina	Tab-on-Disc, 3N, 1 m/s	0.00003	0.39	3
Cr <sub>2</sub> AlC - 20 vol% Ag		Tab-on-Disc, 3N, 1 m/s	0.00007	0.55	
Electrodeposited Ag Coating	Si <sub>3</sub> N <sub>4</sub> balls	Ball-on-Disc, 0.5 N, 0.12 m/s	0.00055	0.4	5
Electrodeposited Ag Coating with Ni Transition Layer		Ball-on-Disc, 0.5 N, 0.12 m/s	0.00008	0.2	
VN	Si <sub>3</sub> N <sub>4</sub> balls	Ball-on-Disc, 2 N, Humid air, 0.11 m/s	NA	0.8	6
VN-28 at% Ag		Ball-on-Disc, 2 N, Humid air, 0.11 m/s	NA	0.32	
VN - 42 at% Ag		Ball-on-Disc, 2 N, Humid air, 0.11 m/s	NA	0.4	
VN-57 at% Ag		Ball-on-Disc, 2 N, Humid air, 0.11 m/s	NA	0.45	
Ti <sub>3</sub> Al/Ag Coatings	AISI52100 steel balls	Ball-on-Disc, 5 N, Air environment, 0.1884 m/s	0.0001	0.3	7
Pure Ti Substrate		Ball-on-Disc, 5 N, Air environment, 0.1884 m/s	0.000042	0.43	
PS-304 Coating (Ag, CaF <sub>2</sub> /BaF <sub>2</sub> eutectic, Cr <sub>2</sub> O <sub>3</sub> hardener in Nichrome matrix)	Inconel X-750	Thrust-washer sliding tests, 25°C, 84 N, 5.4 m/s Powder and sprayed at NASA	0.000119048	0.58	8
Ag	Alumina	Block (Tab) - on - Disc, 5N, 0.5 m/s	0.000049	0.38	This work
Ag - 5 vol% Ti <sub>3</sub> SiC <sub>2</sub>		Block (Tab) - on - Disc, 5N, 0.5 m/s	0.000032	0.38	
Ag - 10 vol% Ti <sub>3</sub> SiC <sub>2</sub>		Block (Tab) - on - Disc, 5N, 0.5 m/s	0.000029	0.35	
Ag - 20 vol% Ti <sub>3</sub> SiC <sub>2</sub>		Block (Tab) - on - Disc, 5N, 0.5 m/s	0.0000041	0.29	
Ag - 30 vol% Ti <sub>3</sub> SiC <sub>2</sub>		Block (Tab) - on - Disc, 5N, 0.5 m/s	0.000025	0.3	

Figures 2.9 shows the SEM evaluation of tribosurfaces of Bi-based MRM after tribological testing. Figures 2.9 a-d show the SEM study of Bi-Al<sub>2</sub>O<sub>3</sub> tribolcouple. Bi sample was riddled with scars from abrasive wear whereas the alumina surface was covered with a uniform tribofilm transferred from the Bi surface. The surface has a tribochemistry with composition A1 (Table 2). The Bi-20 vol% Ti<sub>3</sub>SiC<sub>2</sub> and Al<sub>2</sub>O<sub>3</sub> tribocouple also showed similar features where abrasive wear scars was present on the Bi-20 vol% Ti<sub>3</sub>SiC<sub>2</sub> surface and the Al<sub>2</sub>O<sub>3</sub> surface was covered with tribofilm of chemistry B1 (partially oxidized mixtures of Bi and Ti<sub>3</sub>SiC<sub>2</sub>) and C1 (partially oxidized Bi), respectively (Table 2). Figure 2.10 shows the SEM evaluation of Ag-20 vol% Ti<sub>3</sub>SiC<sub>2</sub> and alumina surfaces. Ag-20 vol% Ti<sub>3</sub>SiC<sub>2</sub> surface was covered with abrasive wear tracks whereas Al<sub>2</sub>O<sub>3</sub> surface was covered with patchy tribofilms. These tribofilms were composed of mildly oxidized Ag and Ti<sub>3</sub>SiC<sub>2</sub> mixtures and had a composition of D1 with no phase separation (Table 2.2).

Table 2.2: Tribochemistry of Different Tribocouples

Composition	Tribochemistry	Ref.
A1	$\text{Bi}_{1\pm 0.035}\text{O}_{0.35\pm 0.22}\{\text{C}_x\}$	This work
B1	$(\text{Bi}_{0.73\pm 0.04}\text{Ti}_{0.18\pm 0.03}\text{Si}_{0.06\pm 0.01})\text{O}_{1.08\pm 0.01}\{\text{C}_x\}$	
C1	$\text{Bi}_{1\pm 0.20}\text{O}_{0.01\pm 0.01}\{\text{C}_x\}$	
D1	$(\text{Ag}_{0.87\pm 0.02}\text{Ti}_{0.04}\text{Si}_{0.09})\text{O}_{0.26\pm 0.04}\{\text{C}_x\}$	
K	$[\text{Ta}_{0.45}\text{Al}_{0.35}\text{Ag}_{0.3}]\text{O}_{1.6}\{\text{C}_x\}$	29
S	$[\text{Ta}_{0.2}\text{Al}_{0.1}\text{Ag}_{0.7}]\text{O}_{0.5}\{\text{C}_x\}$	
T	$[\text{Ta}_{0.45}\text{Al}_{0.2}\text{Ag}_{0.35}]\text{O}_1\{\text{C}_x\}$	

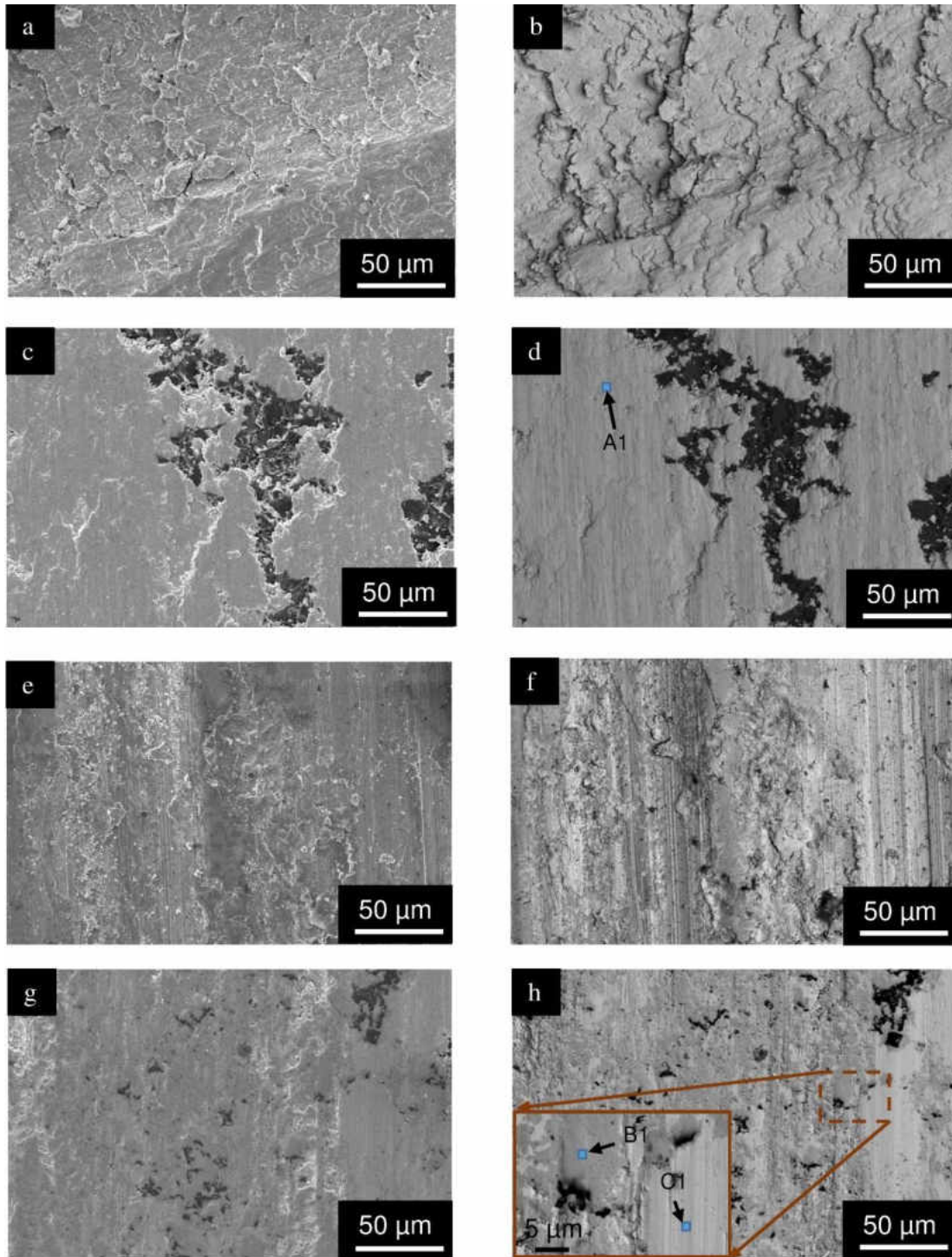


Fig 2.9: SE SEM micrographs of (a) Bi surface, (b) BSE of the same region, (c) alumina counter surface, (d) BSE of the same region, (e) Bi-20 vol% Ti<sub>3</sub>SiC<sub>2</sub> surface, (f) BSE of the same region, (g) alumina countersurface, and (h) BSE of the same region (inset shows the higher magnification of the marked region) after tribological testing.



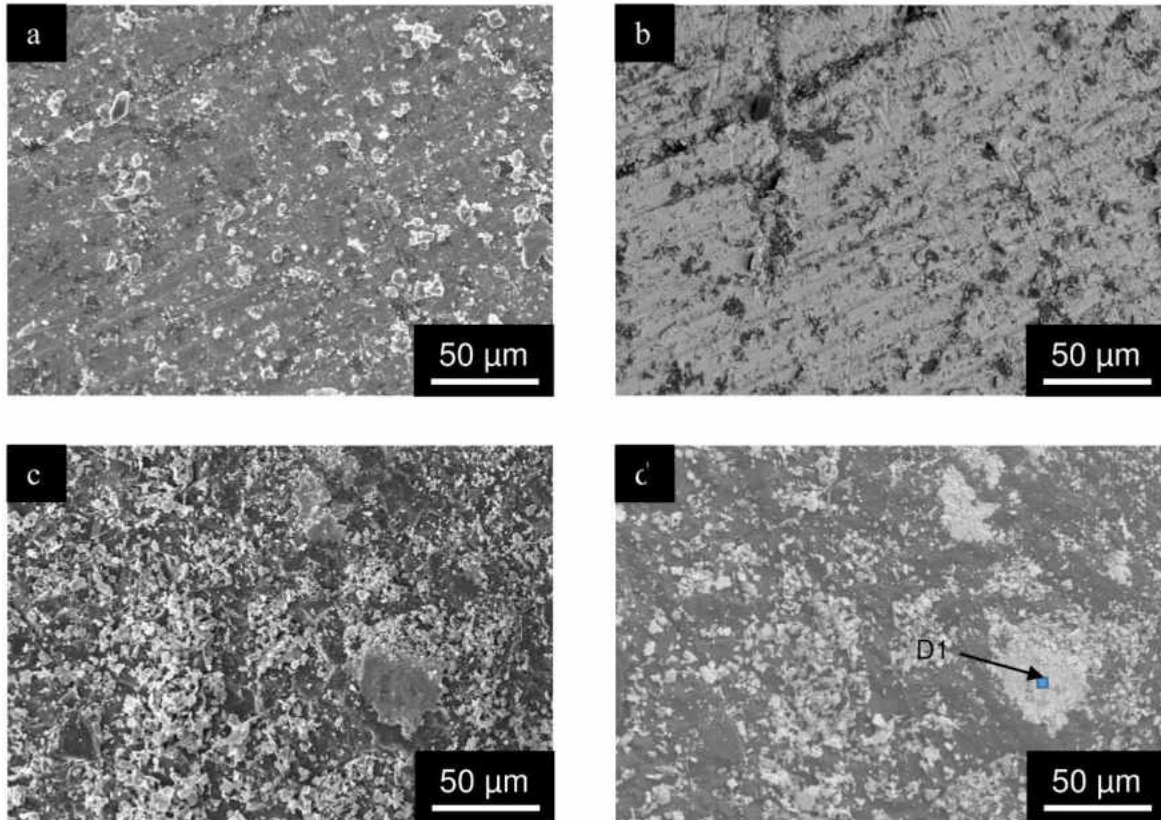


Fig. 2.10: SE SEM micrographs of, (a) Ag-20 vol% Ti<sub>3</sub>SiC<sub>2</sub> surface, (b) BSE of the same region, (c) alumina countersurface, and (d) BSE of the same region.

### 2.3.4 Mechanism of Wear

The tribology of MAX phases and their composites can be understood by studying their tribofilms [1]. Gupta and Barsoum [1] proposed that these tribofilms can be classified into four categories, namely (a) MAX phase surface is the source of triboreactions (Type-I), (b) countersurface is the source of triboreactions (Type-II), (c) both MAX phase or their composites and the tribopartner contributes to the formation of tribofilms (Type-III), and (d) MAX phase based composites contribute predominantly to the triboreactions (Type-IV). These categories can be further divided into sub-categories by documenting the architectures and physical appearance of the tribofilms. The architectures of the tribofilms

were mainly dependent on their degree of oxidation and mechanical integrity like adhesion to the substrate and hardness [1].

According to the evidence presented, the metal-based MRMs are mainly contributing to the formation of tribofilms, thus these tribofilms can be classified into Type IV tribofilms. At this juncture, it is critical to review the Type IV tribofilms. Figure 2.11 shows different types of Type IV tribofilms. Based on the architecture of the tribofilms, the Type IV tribofilms can be further divided into: (a) Type IVa tribofilms are lubricious and chemically homogenous at the microscale [1, 29] (Fig. 2.11a), (b) Type IVb tribofilms are composed of decomposed Ag-rich regions dispersed with different trioxides (Fig. 2.11b) [1, 29], and (c) Type IVc tribofilms were powdery; and this type of tribofilm was first observed during dry sliding of Al-Ti<sub>3</sub>SiC<sub>2</sub> composites against Al<sub>2</sub>O<sub>3</sub> or Zn-Ti<sub>3</sub>SiC<sub>2</sub> composites against Al<sub>2</sub>O<sub>3</sub> [24 - 26] (Fig. 2.11c). Clearly, the tribofilms formed between Bi-based MRMs and alumina and Ag-based MRMs and alumina can be classified as Type IVa as the tribofilms are lubricious and chemical homogenous. This study also shows that the formation of patchy but lubricious tribofilms can be effective in alleviating the WR and reducing  $\mu$  between moving surfaces.

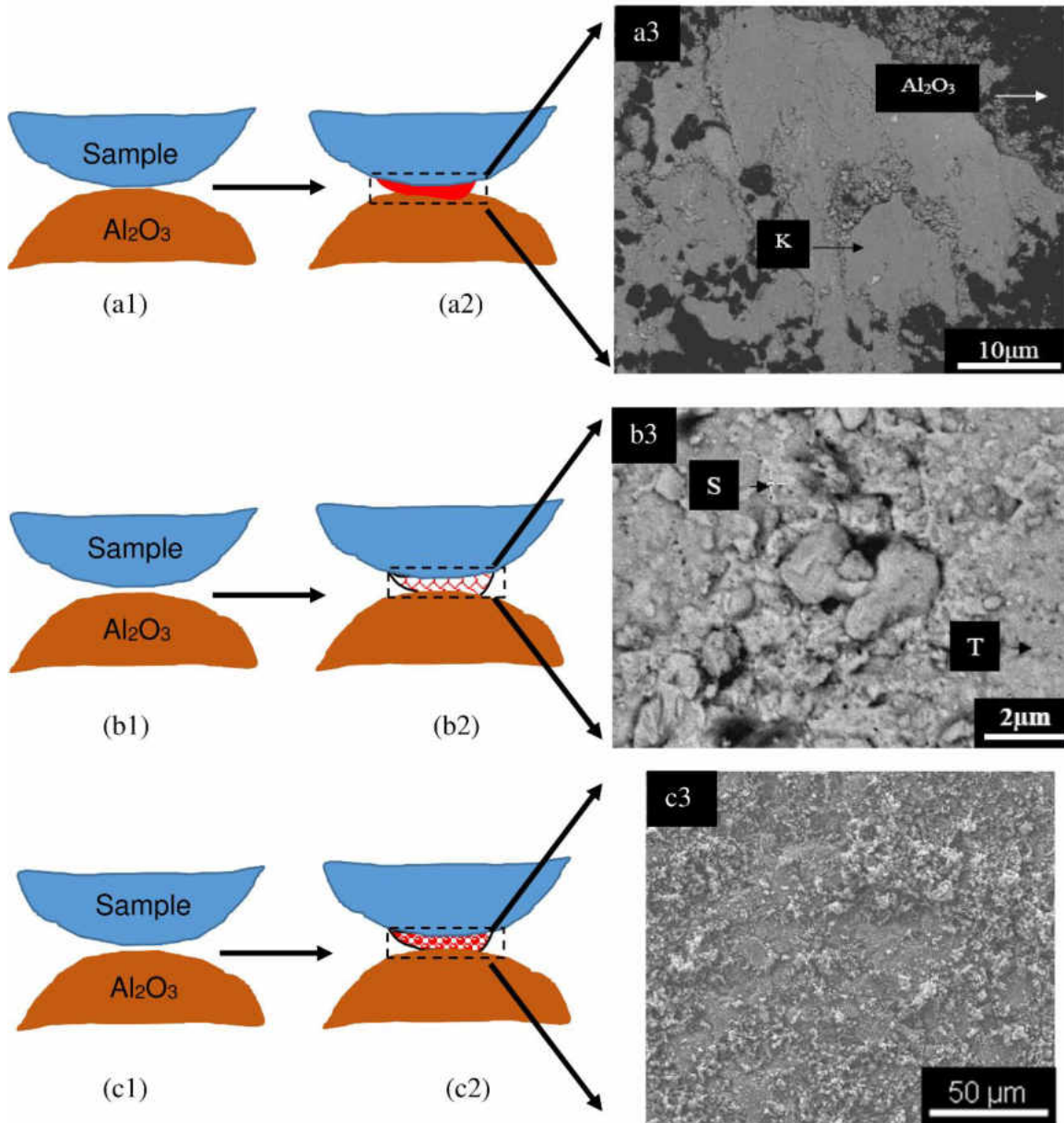


Fig. 2.11: Schematics of (a1) tribocontact, (a2) Type IVa tribofilm, and (a3) SEM micrograph showing a Type IVa tribofilm formed on alumina surface [1, 29]; (b1) tribocontact, (b2) Type IVb tribofilm [2, 28], and (b3) Type IVb tribofilm formed on alumina surface [1]; and (c1) tribocontact, (c2) Type IVc tribofilm, and (c3) Type IVc tribofilm formed on alumina surface [24].

## 2.4 Conclusion

During this study, Bi- and Ag-based MRMs were fabricated for the first time. The addition of  $\text{Ti}_3\text{SiC}_2$  particulates enhanced the hardness and compressive yield strength of both the compositions. For example, in Bi-based MRM systems, the yield strength improved from  $\sim 42$  MPa in Bi to  $\sim 71$  MPa in Bi-30 vol%  $\text{Ti}_3\text{SiC}_2$  (enhancement in strength by  $\sim 1.7$  times). For Ag-based MRM systems, the yield strength improved from  $\sim 47$  MPa in Ag to  $\sim 164$  MPa in Ag- 20 vol  $\text{Ti}_3\text{SiC}_2$  (enhancement in strength by  $\sim 3.5$  times), thereafter, it dropped slightly to 117 MPa in Ag-30 vol%  $\text{Ti}_3\text{SiC}_2$ . As the Bi samples were fabricated by using two different dies, more studies are needed to understand the effect of die size of the physical and mechanical properties of these composites. The addition of  $\text{Ti}_3\text{SiC}_2$  particulates also enhanced the tribological performance. The  $\mu_{\text{mean}}$  decreased gradually from  $\sim 0.38$  in Ag to  $\sim 0.30$  in Ag-30 vol%  $\text{Ti}_3\text{SiC}_2$ . Similarly, the  $\mu_{\text{mean}}$  decreased gradually from  $\sim 0.50$  in Bi to  $\sim 0.41$  in Bi-20 vol%  $\text{Ti}_3\text{SiC}_2$ , thereafter it increased  $\sim 0.53$  in Bi-30 vol%  $\text{Ti}_3\text{SiC}_2$ . Ag-based MRMs showed the lowest WR, more particularly, the WR of Ag decreased from  $4.9 \times 10^{-5} \text{ mm}^3/\text{N.m}$  to  $4.2 \times 10^{-6} \text{ mm}^3/\text{N.m}$  in Ag-20 vol%  $\text{Ti}_3\text{SiC}_2$ , and then increased to  $2.5 \times 10^{-5} \text{ mm}^3/\text{N.m}$  in Ag-30 vol%  $\text{Ti}_3\text{SiC}_2$ . Similarly, in Bi-based MRMs, Bi had a WR of  $0.02 \text{ mm}^3/\text{N.m}$ , and it decreased to  $3 \times 10^{-4} \text{ mm}^3/\text{N.m}$  in Bi-10 vol%  $\text{Ti}_3\text{SiC}_2$ , and marginally increased to  $6 \times 10^{-4} \text{ mm}^3/\text{N.m}$  and  $4.5 \times 10^{-4} \text{ mm}^3/\text{N.m}$  in Bi-20 vol%  $\text{Ti}_3\text{SiC}_2$  and Bi-30 vol%  $\text{Ti}_3\text{SiC}_2$ , respectively. The tribological mechanism was governed by the formation of tribofilms, for example, the tribofilms formed by Bi-based MRMs and Ag-based MRMs against alumina can be classified as Type IVa.

## CHAPTER III

### Synthesis and Tribological Behavior of Bi-Cr<sub>2</sub>AlC Composites

**Abstract (this Chapter has been accepted for publication in 41<sup>st</sup> ICACC Proceedings):**

In this research, we report the synthesis of Bi-Cr<sub>2</sub>AlC composites for the first time by hot pressing. Detailed inspection of the samples by SEM showed the Cr<sub>2</sub>AlC particulates are well dispersed in the Bi-matrix. The addition of Cr<sub>2</sub>AlC particulates had a beneficial effect on the mechanical and tribological behavior. For example, the yield strength increased by 1.8 times from ~40 MPa in Bi to ~72 MPa in Bi-30%Cr<sub>2</sub>AlC. The addition of 10 vol% Cr<sub>2</sub>AlC was able to decrease the WR of Bi-composites by ~100 times as compared to the Bi metal. Detailed SEM investigations showed the anti-wear properties of these composites are due to the formation of smooth and lubricious tribofilms.

### 3.1 Introduction

Bi is an important metal for solid lubrication and hot forming as it can be considered green alternative to Pb and has been studied for solid lubrication and hot forming [1-2]. As reported in Chapter 2 in this thesis,  $Ti_3SiC_2$  can be added as reinforcing additive in Bi which improved the mechanical and tribological behavior of Bi. As a background,  $Ti_3SiC_2$  and  $Cr_2AlC$  belongs to a family of compound called  $M_{n+1}AX_n$  (MAX) phases (over 70+ phases), where  $n = 1-3$ , M is an Early Transitional Metal, A is a Group A element (mostly groups 13 and 14), and X is C or N. These solids have attracted a lot of attention due their excellent properties like solid lubrication, damage tolerance, thermal shock resistance and machinability [4-8]. Gupta [13] studied  $Cr_2AlC$  tribological behavior at room temperature and  $550\text{ }^\circ\text{C}$  against alumina and Inconel 718 substrates and found a negligible wear rate at  $550\text{ }^\circ\text{C}$  and quite a high wear rate at room temperature. Recently, Gupta et al. [9-11] also demonstrated that the addition of  $Ti_3SiC_2$  particulates enhanced the mechanical and tribological performance of different technologically important metals like Al-matrix, Sn-matrix, and Zn-matrix composites. The authors referred to this new generation of composites as MRM (Metal Reinforced with MAX) as 5-30 vol%  $Ti_3SiC_2$  was used to reinforce the metal matrix. In this research, the effect of  $Cr_2AlC$  particulates on the mechanical and tribological behavior of Bi will be studied.

### 3.2 Experimental Methods

Cr (-325 mesh, Sigma-Aldrich, St. Louis, MO), Al (-325 mesh, Alfa Aesar, Haverhill, MA), and C (-325 mesh, Alfa Aesar, Haverhill, MA) powders were mixed in the molar ratio of 2:1.1:1 in a ball mill (8000 M mixer Mill, SPEX SamplePrep, Metuchen, NJ) for 5 minutes. The powders were cold pressed then heated at  $10\text{ }^\circ\text{C}/\text{min}$  to the desired

temperature, and then sintered at 1350 °C for 4 h in a tube furnace with Ar gas flowing through the furnace. The phase pure Cr<sub>2</sub>AlC powder was then mixed with calculated concentrations of Bi powders (-100 mesh, Sigma Aldrich, St. Louis, MO)) by dry ball milling for 5 minutes. All the powders were then poured in a die. Bi-based were difficult to machine as they were soft at low concentration of Ti<sub>3</sub>SiC<sub>2</sub> or brittle at 30 vol% Ti<sub>3</sub>SiC<sub>2</sub>, thus, in order to minimize machining, two sets of Bi-based compositions were fabricated by using ~12.7 mm (EQ-Die-12D-B, MTI Corporation, Richmond, CA) and ~6.35 mm (EQ-Die-06D, MTI Corporation, Richmond, CA) dies for hot pressing. The Bi-based compositions were sintered in atmospheric air by hot pressing (HP) with a uniaxial compressive stress of ~201 MPa (~12.7 mm die) or ~251 MPa (~6.35 mm) at 290 °C for 5 minutes. Samples from the former set were used for hardness and tribology studies where samples from the latter set were used for mechanical performance. Composites were allowed to cool in the HP to room temperature (RT) before characterization. For comparison, samples of pure Bi was also fabricated by following the above mentioned method. Bi-based MRM composites were fabricated by adding 10 vol% (Bi-10%Cr<sub>2</sub>AlC), 20 vol% (Bi-20%Cr<sub>2</sub>AlC), and 30 vol% (Bi-30% Cr<sub>2</sub>AlC) Cr<sub>2</sub>AlC in the Bi- matrix.

The methodology for determining relative density and porosity of the compacts is reported in Chapter 2. Briefly, the relative density was determined by normalizing the experimental density with theoretical density. Thereafter, the porosity is calculated based on the methodology explained in Chapter 2. A mechanical testing unit (Shimadzu AD-IS UTM, Shimadzu Scientific Instruments Inc., Columbia, MD) applied a deflection rate of 1 mm/min to evaluate the strength of samples during compression by testing a set of 3 samples for each composition. In this work, stress versus displacement plots are reported

due to the experimental limitations which did not allow for accurate measurement of the actual strain during mechanical testing. During this study, the yield strength is defined as the stress at which the stress versus displacement plot transitions from the linear to non-linear regime where the linear region of the composites had a regression fitting of  $R^2 > 0.95$ . An average of 3 yield strength results was used to calculate average strength. Vicker's micro-hardness indenter (Mitutoyo HM-112, Mitutoyo Corporation, Aurora, IL) was used to measure the hardness of the polished samples ( $R_a < 1 \mu\text{m}$ ). Bi-based MRMs were tested by loading the samples at 0.49 N for 12 s and an average of five readings for each composite system is reported in this study.

The tribological behavior of the samples were tested by using a block (tab)-on-disc tribometer (CSM Instruments SA, Peseux, Switzerland) at 5 N ( $\sim 0.3 \text{ MPa}$ ), 50 cm/s linear speed, 1000 m sliding distance, and  $\sim 10 \text{ mm}$  track radius against alumina disks (AL-D-42-2, AdValue Technology, Tucson, AZ). Bi samples were tested for only  $\sim 80 \text{ m}$  as they had higher wear as compared to Bi-based MRMs which were cycled for  $\sim 1000 \text{ m}$  [3]. For tribological testing, the blocks ( $\sim 4 \text{ mm} \times \sim 4 \text{ mm} \times \sim 3 \text{ mm}$ ) were polished to a  $\sim 1 \mu\text{m}$  finish. Alumina disks were also polished to a  $\sim 1 \mu\text{m}$  finish. A surface profilometer (Surfcom 480A, Tokyo Seimitsu Co. Ltd., Japan) was used to confirm that all the samples had a  $R_a < 1 \mu\text{m}$ . For each composition, three experimental studies for tribological studies were performed. The average of the individual mean results reported from the three data set was calculated and reported in the text as  $\mu_{\text{mean}}$ . The specific wear rate (WR) was then calculated from:

$$WR = (m_i - m_f) / (\rho \cdot N \cdot d)$$



where,  $m_i$  is the initial mass,  $m_f$  is the final mass,  $\rho$  is density of the composite,  $N$  is the applied load, and  $d$  is the total distance traversed by the tab during the tribology testing [9-11].

Secondary electron (SE) and backscattered electrons (BSE) images were obtained by using a JEOL JSM-6490LV Scanning Electron Microscope (JEOL USA, Inc., Peabody, Massachusetts) and X-ray information was obtained via a Thermo Nanotrace Energy Dispersive X-ray detector with NSS-300e acquisition engine. For microscopy analysis, alumina samples were coated with Au/Pd by using a Balzers SCD 030 sputter coater (BAL-TEC RMC, Tucson AZ USA), and then mounted on aluminum mounts. The tribosurfaces, especially sub-stoichiometric oxides, could very well contain C which is very difficult to determine experimentally by X-ray analysis. If a region is determined to be chemically uniform at the micron level then it will be identified with two asterisks as \*microconstituent\* to emphasize that these areas are not necessarily single phases. In addition, the presence of C in these tribofilms will be shown by adding {C<sub>x</sub>} in the composition [12].

### **3.3 Results and Discussion**

#### **3.3.1 Microstructure and Phase Analysis**

Figure 3.1 shows the microstructure of Bi-Cr<sub>2</sub>AlC composites. In all the cases, Cr<sub>2</sub>AlC particles are well dispersed in the Bi-matrix with minimal reaction. Figure 3.2a plots the variation of hardness as a function of Cr<sub>2</sub>AlC and Ti<sub>3</sub>SiC<sub>2</sub> content. In both cases, the addition of harder MAX phase constituent increased the hardness of the matrix. Figure 3.2b shows the porosity of the composites as a function of the MAX phase content. In both cases, the porosity increased with the addition of higher vol% of MAX phases which

shows that it is difficult to densify the compacts as the concentration of both  $\text{Cr}_2\text{AlC}$  and  $\text{Ti}_3\text{SiC}_2$  [3] is increased inside the matrix. The same behavior was observed during the processing of Al- [9], Sn- [10], and Zn- [11] based MRM composites. Thus, it can be concluded that higher pressures and/or temperature are needed as compared to the pristine metal samples when the amount of MAX phases are increased in the metal matrix.

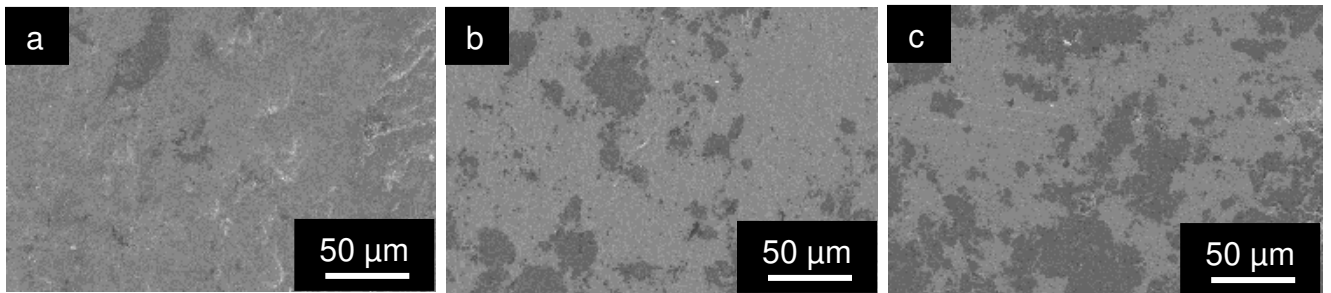


Figure 3.1: SEM SE microstructure of (a) Bi-10% $\text{Cr}_2\text{AlC}$ , (b) Bi-20% $\text{Cr}_2\text{AlC}$ , and (c) Bi-30% $\text{Cr}_2\text{AlC}$ .

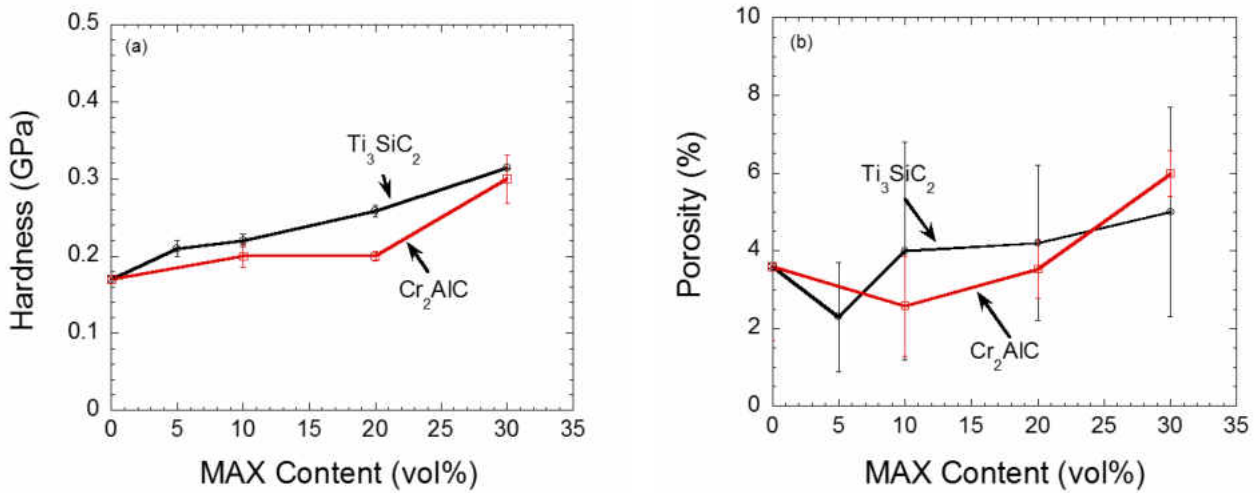


Figure 3.2: Plot of (a) hardness, and (b) porosity versus MAX content.

### 3.3.2 Mechanical Performance of MRMs

Figure 3.3a plots the compressive strength versus displacement of Bi-Cr<sub>2</sub>AlC composites. The yield strength gradually improved as the concentration of Cr<sub>2</sub>AlC was increased in the Bi-matrix. Figure 3.3b compares the yield strength of Bi-Ti<sub>3</sub>SiC<sub>2</sub> and Bi-Cr<sub>2</sub>AlC composites. Both the composites showed similar trend and the addition of MAX

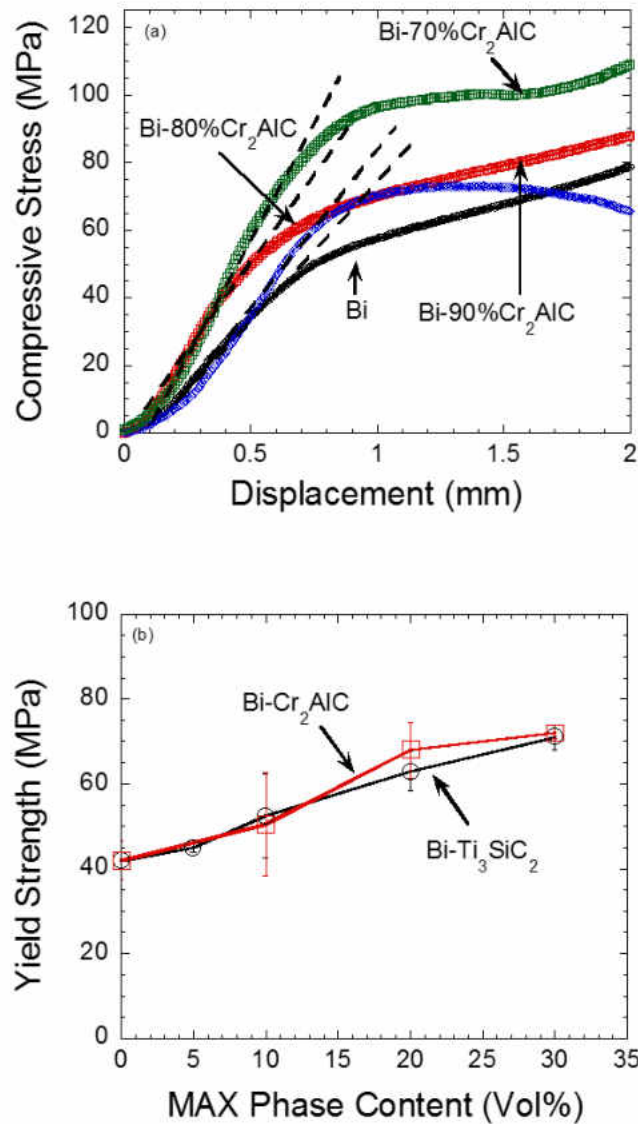


Figure 3.3: Plot of (a) compressive stress versus displacement, and (b) yield strength versus MAX phase content of different Bi-MAX composites.

phases enhanced the yield strength of Bi-matrix, for example, the yield strength of Bi-Cr<sub>2</sub>AlC composites increased from ~40 MPa in Bi to ~72 MPa in Bi-30%Cr<sub>2</sub>AlC (~1.8 times increased in enhancement). Furthermore, this study shows that Cr<sub>2</sub>AlC particulates can be as effective as Ti<sub>3</sub>SiC<sub>2</sub> in enhancing the yield strength of metal matrix.

### 3.3.3 Tribological Behavior of MRMs

Figure 3.4a plots the  $\mu_{\text{mean}}$  of Bi-Cr<sub>2</sub>AlC and Bi-Ti<sub>3</sub>SiC<sub>2</sub> composites. In general, Bi-Ti<sub>3</sub>SiC<sub>2</sub> composites showed lower friction coefficient than Bi-Cr<sub>2</sub>AlC composites. Figure 3.4b plots the comparison of WR of Bi-Cr<sub>2</sub>AlC and Bi-Ti<sub>3</sub>SiC<sub>2</sub> composites. Both the composites showed similar trends in WR. For example, the WR of Bi decreased from ~0.02 mm<sup>3</sup>/N.m to ~2 x 10<sup>-4</sup> mm<sup>3</sup>/N.m in Bi-10%Cr<sub>2</sub>AlC, then increased to ~9 x 10<sup>-4</sup> and ~7 x 10<sup>-4</sup> mm<sup>3</sup>/N.m in Bi-20%Cr<sub>2</sub>AlC and Bi-30%Cr<sub>2</sub>AlC, respectively. In other words, the addition of 10 vol% Cr<sub>2</sub>AlC particulates decreased the WR of the composites by ~100 times. This study demonstrates that Cr<sub>2</sub>AlC can be as effective an anti-wear additive as Ti<sub>3</sub>SiC<sub>2</sub>. At this juncture, it is not clear why the  $\mu_{\text{mean}}$  of Bi-Cr<sub>2</sub>AlC is higher as compared to Bi-Ti<sub>3</sub>SiC<sub>2</sub> composites. Detailed investigations are needed to understand the exact mechanism. Figure 3.5a shows the surface of Bi-20%Cr<sub>2</sub>AlC after tribological testing. Figures 3.5b-c show the tribofilms formed due to tribooxidation of Bi-20%Cr<sub>2</sub>AlC on the alumina surface. The tribofilms were uniform, for example, the chemistry of two regions are  $(\text{Bi}_{0.71\pm0.07}\text{Cr}_{0.18\pm0.01}\text{Al}_{0.11\pm0.01})\text{O}_{0.75\pm0.09}\{\text{C}_x\}$  and  $(\text{Bi}_{0.54\pm0.01}\text{Cr}_{0.19\pm0.02}\text{Al}_{0.14\pm0.01})\text{O}_{0.93\pm0.03}\{\text{C}_x\}$ , respectively. Like Bi-Ti<sub>3</sub>SiC<sub>2</sub> composites [3], the Bi-Cr<sub>2</sub>AlC composites are mainly contributing towards the formation of tribofilms. According to the classification proposed by Gupta and Barsoum [12], the tribofilms formed

between Bi-based MRMs and alumina can be classified as Type IVa as the tribofilms are lubricious and chemical homogenous.

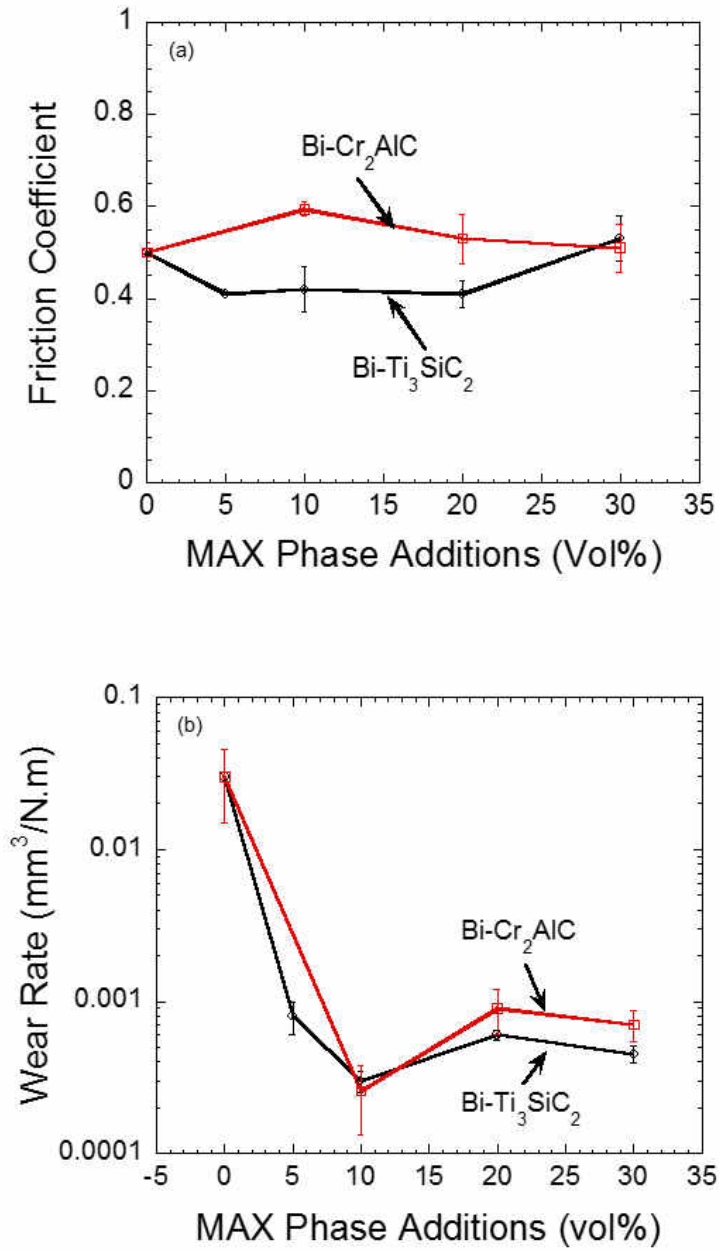


Figure 3.4: Plot of (a) friction coefficient, and (b) wear rate versus MAX phase additions.

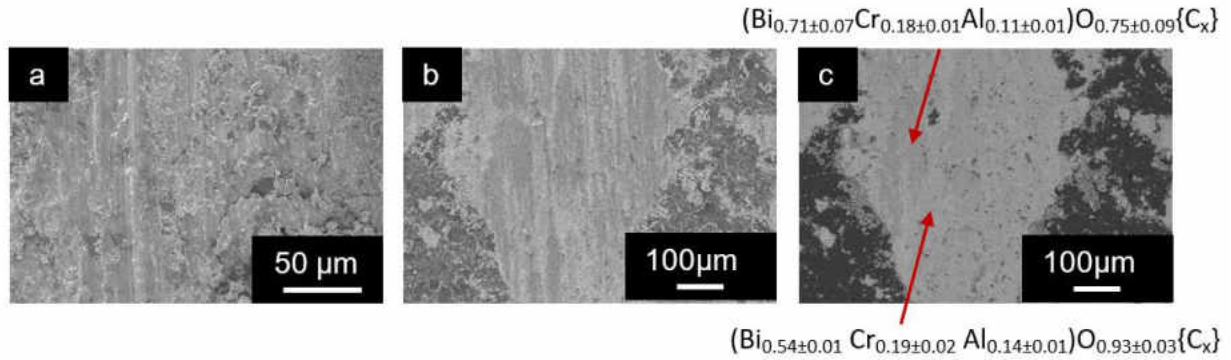


Figure 3.5: SEM SE micrographs of (a) Bi-20%Cr<sub>2</sub>AlC, (b) alumina surface, and (c) BSE image of the same region after tribological testing.

### 3.4 Conclusion

Bi-Cr<sub>2</sub>AlC composites were fabricated for the first time by hot pressing. The addition of Cr<sub>2</sub>AlC particulates increased the yield strength of Bi-Cr<sub>2</sub>AlC composites increased from ~40 MPa in Bi to ~72 MPa in Bi-30%Cr<sub>2</sub>AlC (~1.8 times increased in yield strength). The WR of Bi decreased from 0.02 mm<sup>3</sup>/N.m to ~2 × 10<sup>-4</sup> mm<sup>3</sup>/N.m in Bi-10%Cr<sub>2</sub>AlC, then increased to ~9 × 10<sup>-4</sup> and ~7 × 10<sup>-4</sup> mm<sup>3</sup>/N.m in Bi-20%Cr<sub>2</sub>AlC and Bi-30%Cr<sub>2</sub>AlC, respectively. In other words, the addition of 10 vol% Cr<sub>2</sub>AlC particulates can decreased the WR of the composites by ~100 times. Type IVa (smooth and lubricious) tribofilms was observed on the alumina surfaces.

## CHAPTER IV

### Synthesis and Tribological Behavior of Al-V<sub>2</sub>AlC, Al-Ti<sub>3</sub>SiC<sub>2</sub> and Al-Cr<sub>2</sub>AlC Composites (Current Research Progress)

#### Abstract:

This chapter reports the current progress of synthesis and tribological behavior of Al-V<sub>2</sub>AlC, Al-Ti<sub>3</sub>SiC<sub>2</sub> and Al-Cr<sub>2</sub>AlC composites. The addition of MAX phase particulates enhanced the hardness and compressive yield strength of all compositions. The yield strength is increased gradually from ~118 MPa in pristine Al to ~194 MPa in Al-30%V<sub>2</sub>AlC. Furthermore, the addition of Ti<sub>3</sub>SiC<sub>2</sub> and Cr<sub>2</sub>AlC increased the yield point gradually and reached ~194 MPa and 211 MPa for Al-30%Ti<sub>3</sub>SiC<sub>2</sub> and Al-30%Cr<sub>2</sub>AlC, respectively. In other words, the addition of 30% MAX phase particulates showed an enhancement in strength by ~1.7 times. The study showed that the addition of MAX phase particulates also had a remarkable effect on tribological performance. All the samples were tested by block (tab)-on-disk method. The pure Al samples showed  $\mu_{\text{mean}}$  value of 0.55. However, the addition of Ti<sub>3</sub>SiC<sub>2</sub> and V<sub>2</sub>AlC particulates decreased  $\mu_{\text{mean}}$  to below 0.50. On the other hand, the WR of Al decreased from 0.25 mm<sup>3</sup>/N.m to 1.1 X 10<sup>-3</sup> mm<sup>3</sup>/N.m in Al-30%V<sub>2</sub>AlC. Similarly, the addition of Ti<sub>3</sub>SiC<sub>2</sub> decreased the WR to 7.3 X 10<sup>-4</sup> mm<sup>3</sup>/N.m in the Al-10%Ti<sub>3</sub>SiC<sub>2</sub>, thereafter it increased to 1.6 X 10<sup>-3</sup> mm<sup>3</sup>/N.m and 2.1 X 10<sup>-3</sup> mm<sup>3</sup>/N.m in the Al-20%Ti<sub>3</sub>SiC<sub>2</sub> and Al-30%Ti<sub>3</sub>SiC<sub>2</sub>, respectively.

## 4.1 Introduction

Aluminum-based materials can be used in different applications due to their promising properties under different applications. Most importantly, Al has good strength-to-weight ratio, high corrosion resistance, and good thermal and electrical conduction [1]. Thus, aluminum based materials have been used to replace crucial components for aerospace and automotive industries which leads to lower fuel and power consumption [1]. However, Al-based materials showed a poor tribological behavior where they showed high wear rates comparing with other soft metals like Ag and Sn [2-4]. Several attempts were approached to reinforce Al with different ceramics to improve tribological behavior of Al based materials. Jinfeng et al. [5] studied the effect of adding Graphite to Al based material and successfully decreased the friction coefficient and wear rate significantly. However, the addition of graphite resulted in significant reduction in the yield strength. Furthermore, it's well knowing that the presence of water or hydrocarbons are essential for graphite to be an effective solid lubricant [6]. Hard ceramics like  $\text{Al}_2\text{O}_3$ , SiC and  $\text{B}_4\text{C}$  showed significant reduction in wear rate; however, it also reported that there is variation in friction coefficient [7-9]. Recently, Gupta et al. [2-4] demonstrated that the addition of  $\text{Ti}_3\text{SiC}_2$  particulates enhanced the mechanical and tribological performance of different technologically important metals like Al-matrix, Sn-matrix, and Zn-matrix composites. Gupta et al. [2] used liquid phase pressureless sintering for fabricating Al-based MRMs composites. In this research, the effect of adding  $\text{V}_2\text{AlC}$ ,  $\text{Ti}_3\text{SiC}_2$  and  $\text{Cr}_2\text{AlC}$  particulates on the mechanical and tribological behavior of Al via hot pressing will be studied.



## 4.2 Experimental Methods

V (-325 mesh, Sigma-Aldrich, St. Louis, MO), Al (-325 mesh, Alfa Aesar, Haverhill, MA), and C (-325 mesh, Alfa Aesar, Haverhill, MA) powders were mixed in the molar ratio of 2:1.2:1 in a ball mill (8000 M mixer Mill, SPEX SamplePrep, Metuchen, NJ) for 10 minutes. The powders were cold pressed then heated at 10 °C/min to the desired temperature, and then sintered at 1550 °C for 2 h in a tube furnace with Ar gas flowing through the furnace. Cr (-325 mesh, Sigma-Aldrich, St. Louis, MO), Al (-325 mesh, Alfa Aesar, Haverhill, MA), and C (-325 mesh, Alfa Aesar, Haverhill, MA) powders were mixed in the molar ratio of 2:1.1:1 in a ball mill (8000 M mixer Mill, SPEX SamplePrep, Metuchen, NJ) for 5 minutes. The powders were cold pressed then heated at 10 °C/min to the desired temperature, and then sintered at 1350 °C for 4 h in a tube furnace with Ar gas flowing through the furnace.

The phase pure  $V_2AlC$ ,  $Cr_2AlC$  and  $Ti_3SiC_2$  (-325 mesh, Kanthal, Hallstahammar, Sweden) powder was then mixed with calculated concentrations of Al powders (-325 mesh, Alfa Aesar, Haverhill, MA) by dry ball milling for 5 minutes. All the powders were then poured in a die. In order to minimize machining, two sets of Al-based compositions were fabricated by using ~12.7 mm (EQ-Die-12D-B, MTI Corporation, Richmond, CA) and ~6.35 mm (EQ-Die-06D, MTI Corporation, Richmond, CA) dies for hot pressing. The Al-based compositions were sintered in atmospheric air by hot pressing (HP) with a uniaxial compressive stress of ~201 MPa at 450 °C for 5 minutes. Composites were allowed to cool in the HP to room temperature (RT) before characterization. Samples from the former set were used for hardness and tribology studies where samples from the latter set were used for mechanical performance. For comparison, samples of pure Al were

also fabricated by following the above mentioned method. Al-based MRM composites were fabricated by adding 10 vol%, 20 vol%, and 30 vol% of the MAX phases to produce Al- $V_2AlC$ , Al- $Cr_2AlC$  and Al- $Ti_3SiC_2$  composites as shown in table 4.1.

Table 4.1: Compositions Table

Al vol%	MAX Phase vol%	Composition name
100	0	Al
90	10 ( $V_2AlC$ )	Al-10% $V_2AlC$
80	20 ( $V_2AlC$ )	Al-20% $V_2AlC$
70	30 ( $V_2AlC$ )	Al-30% $V_2AlC$
90	10 ( $Cr_2AlC$ )	Al-10% $Cr_2AlC$
80	20 ( $Cr_2AlC$ )	Al-20% $Cr_2AlC$
70	30 ( $Cr_2AlC$ )	Al-30% $Cr_2AlC$
90	10 ( $Ti_3SiC_2$ )	Al-10% $Ti_3SiC_2$
80	20 ( $Ti_3SiC_2$ )	Al-20% $Ti_3SiC_2$
70	30 ( $Ti_3SiC_2$ )	Al-30% $Ti_3SiC_2$

The methodology for determining relative density and porosity of the compacts is reported in Chapter 2. Briefly, the relative density was determined by normalizing the experimental density with theoretical density. Please refer for Chapter 2 for detailed experimental procedure.

## 4.3 Results and Discussion

### 4.3.1 Mechanical Performance of Al-MAX Composites

Figure 4.1 shows the porosity of the composites as a function of the MAX phase content. In the case of adding  $\text{Ti}_3\text{SiC}_2$  and  $\text{Cr}_2\text{AlC}$ , the porosity increased with the addition of higher vol% of MAX phases which shows that it is difficult to densify the compacts as the concentration of both  $\text{Cr}_2\text{AlC}$  and  $\text{Ti}_3\text{SiC}_2$  is increased inside the matrix. The same behavior was observed in the previous chapters. It had also noted during the processing of Al- [2], Sn- [3], and Zn- [4] based MRM composites. However, the addition of  $\text{V}_2\text{AlC}$  particles did not have the same effect and the porosity was almost similar to the pristine aluminum. Hu et al., [15] reported that  $\text{V}_2\text{AlC}$  is relatively softer than  $\text{Cr}_2\text{AlC}$  and  $\text{Ti}_3\text{SiC}_2$  and thus has less effect on densification process of Al up to 30% $\text{V}_2\text{AlC}$ . For example, Hu et al., [15] reported that the hardness of  $\text{V}_2\text{AlC}$  is less than 2.9 GPa whereas the hardness of  $\text{Cr}_2\text{AlC}$  is  $\sim 3.5$  GPa. This was also true in our current research where the hardness of Al- $\text{V}_2\text{AlC}$  composites is relatively lower than the hardness of Al- $\text{Ti}_3\text{SiC}_2$  or Al- $\text{Cr}_2\text{AlC}$  composites as shown below.

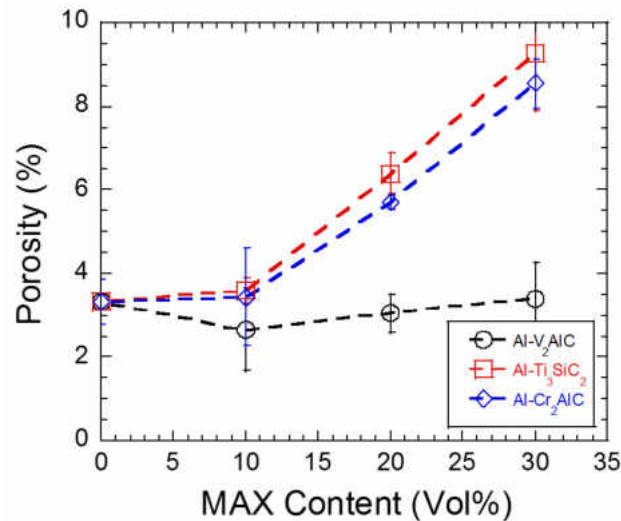


Figure 4.1: Plot of porosity versus MAX phase content.

Figure 4.2 plots the variation of hardness as a function of MAX phase content. In Al-V<sub>2</sub>AlC system, the hardness increased gradually from ~0.46 GPa in Al to ~0.58 GPa in Al-30%V<sub>2</sub>AlC. Similarly, in Al-Cr<sub>2</sub>AlC composites, the hardness increased as the Cr<sub>2</sub>AlC content increased and reached to ~0.60 GPa in Al-30%Cr<sub>2</sub>AlC. Hardness is also increased from ~0.46 GPa in Al to 0.58 GPa in Al-20%Ti<sub>3</sub>SiC<sub>2</sub>. Thereafter, it decreased slightly to ~0.56 GPa Al-30%Ti<sub>3</sub>SiC<sub>2</sub>. In general, the addition of hard MAX phase particulates increased the hardness of the composites, but the presence of porosity in samples account for the slight decreased in hardness of Al-30%Ti<sub>3</sub>SiC<sub>2</sub> as compared to Al-20%Ti<sub>3</sub>SiC<sub>2</sub>. A similar trend was also observed in Sn- [3], Zn- [4] and Ag- [16] based MRM composites.

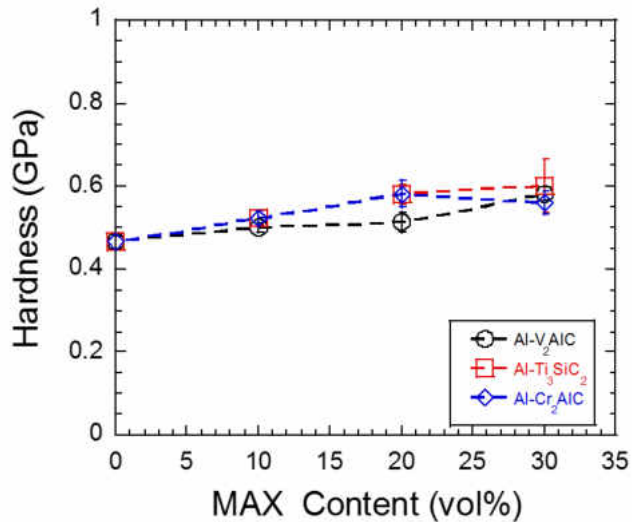


Figure 4.2: Plot of hardness versus MAX phase content.

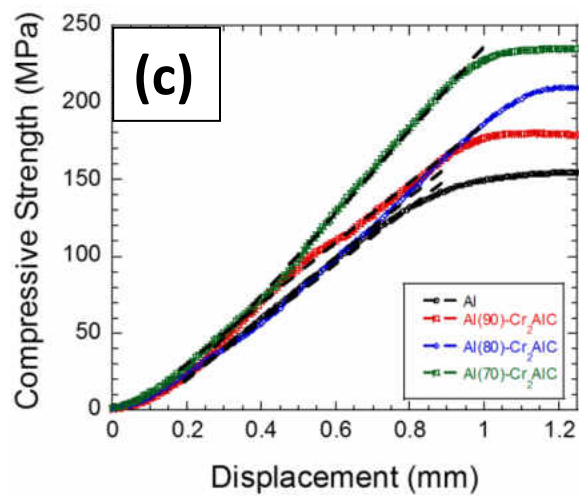
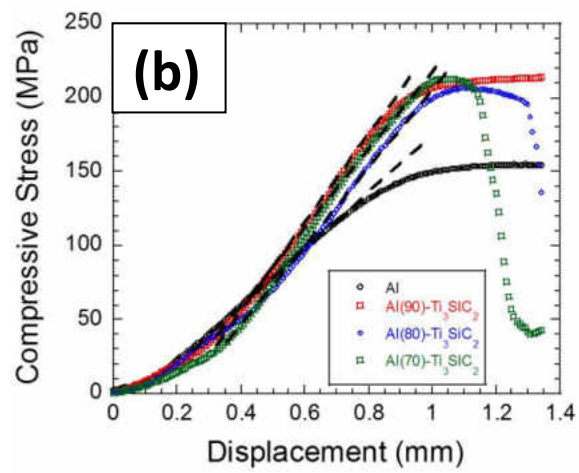
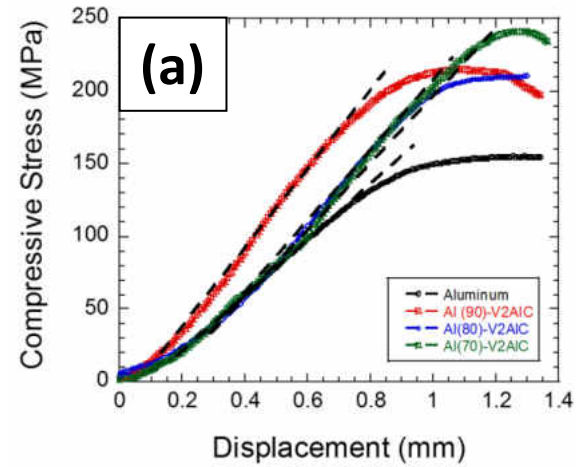


Figure 4.3: Plot of compressive stress versus displacement (a) Al-V<sub>2</sub>A1C, (b) Al-Ti<sub>3</sub>SiC<sub>2</sub>, (c) Al-Cr<sub>2</sub>A1C

Figures 4.3a-c plot the compressive strength versus displacement plots of Al-based composites. All samples showed gradual failure under different MAX phase concentrations. However, brittle failure is observed in Al-20%Ti<sub>3</sub>SiC<sub>2</sub> and Al-30%Ti<sub>3</sub>SiC<sub>2</sub> (Fig. 4.3b). Even though, in all the cases, the compressive yield strength is improved as the concentration of MAX phase particulates is increased in the matrix (Fig. 4.4). The yield strength improved from ~118 MPa in Al to ~194 MPa in Al-30%V<sub>2</sub>AlC. Furthermore, the addition of Ti<sub>3</sub>SiC<sub>2</sub> and Cr<sub>2</sub>AlC increased the yield point gradually and reached to ~194 MPa and ~211 MPa for the Al-30%Ti<sub>3</sub>SiC<sub>2</sub> and Al-30%Cr<sub>2</sub>AlC, respectively. In other words, the addition of 30% MAX phase particulates showed an enhancement in strength of ~1.7 times.

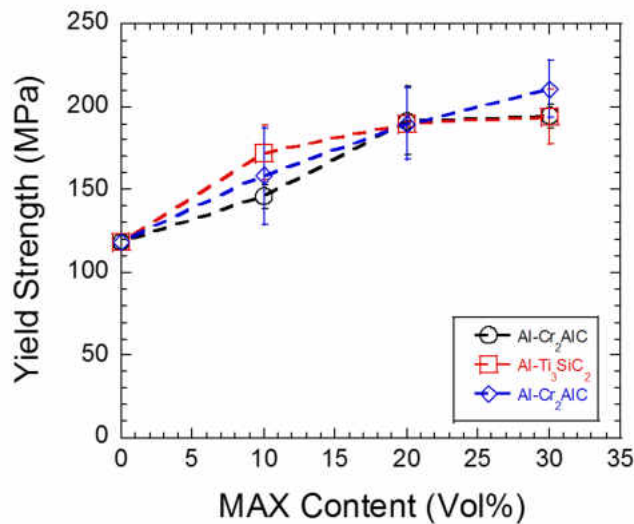


Figure 4.4: Plot of yield strength versus MAX phase content of different Al-MAX phase composites.

### 4.3.2 Tribological Behavior of MRMs

Figure 4.5 plots the  $\mu_{\text{mean}}$  of Al-V<sub>2</sub>AlC, Al-Ti<sub>3</sub>SiC<sub>2</sub> and Al-Cr<sub>2</sub>AlC composites. The pure Al samples showed  $\mu_{\text{mean}}$  value of 0.55. However, the addition of V<sub>2</sub>AlC and Ti<sub>3</sub>SiC<sub>2</sub> particulates decreased  $\mu_{\text{mean}}$  to below than 0.50. Both composites showed almost similar trend where the addition of 10% of V<sub>2</sub>AlC or Ti<sub>3</sub>SiC<sub>2</sub> reduce the  $\mu_{\text{mean}}$  to 0.46 and

thereafter it increased slightly as the concentration increased to 20% and 30%. On the other hand, the addition of  $\text{Cr}_2\text{AlC}$  increased  $\mu_{\text{mean}}$  and same effect was also observed when  $\text{Cr}_2\text{AlC}$  particulates were added to bismuth matrix. Figure 4.6 plots the comparison of WR of Al- $\text{V}_2\text{AlC}$ , Al- $\text{Ti}_3\text{SiC}_2$  and Al- $\text{Cr}_2\text{AlC}$  composites. the WR of Al decreased from  $0.25 \text{ mm}^3/\text{N.m}$  to  $1.1 \times 10^{-3} \text{ mm}^3/\text{N.m}$  in Al-30% $\text{V}_2\text{AlC}$ . Similarly, the addition of  $\text{Ti}_3\text{SiC}_2$  decreased the WR to  $7.3 \times 10^{-4} \text{ mm}^3/\text{N.m}$  in the Al-10% $\text{Ti}_3\text{SiC}_2$ , thereafter it increased to  $1.6 \times 10^{-3} \text{ mm}^3/\text{N.m}$  and  $2.1 \times 10^{-3} \text{ mm}^3/\text{N.m}$  in the Al-20% $\text{Ti}_3\text{SiC}_2$  and Al-30% $\text{Ti}_3\text{SiC}_2$ , respectively. The addition of  $\text{Cr}_2\text{AlC}$  at different concentrations retained almost similar WR values  $\sim (8-10) \times 10^{-4} \text{ mm}^3/\text{N.m}$ . High porosity at high concentrations in Al- $\text{Ti}_3\text{SiC}_2$  comparing with Al- $\text{V}_2\text{AlC}$  could account for high WR and lead to form a less effective film. Gupta [6] showed that  $\text{Ti}_3\text{SiC}_2$  is less lubricious and exhibits high wear rate at room temperature. Thus, increasing  $\text{Ti}_3\text{SiC}_2$  content beyond certain concentration has more drastic effect. Same behavior was observed in Sn- [3], Zn- [4] and Ag- [16] based MRM composites. On the other hand, it can be concluded that  $\text{V}_2\text{AlC}$  is more effective in lowering wear rate at room temperature. Further studies are need to understand the exact mechanism.

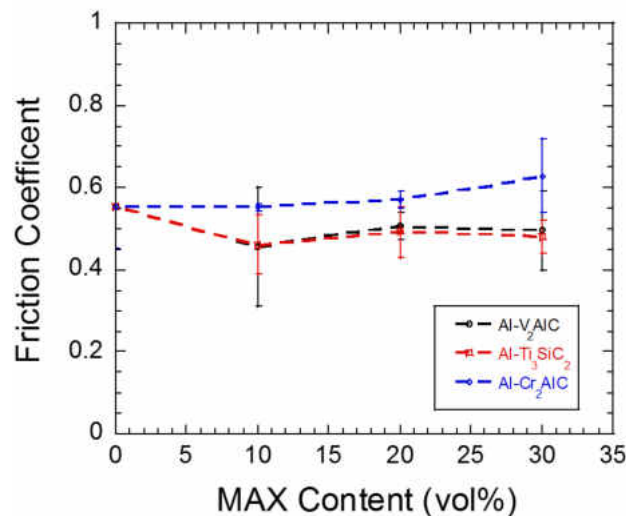


Figure 4.5: Plot of friction coefficient versus MAX phase additions.

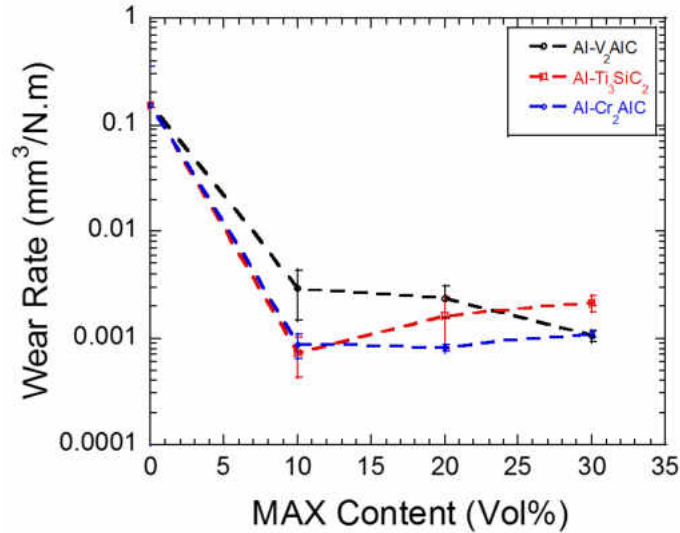


Figure 4.6: Plot of wear rate versus MAX phase additions

#### 4.4 Conclusion

Al-V<sub>2</sub>AlC, Al-Ti<sub>3</sub>SiC<sub>2</sub> and Al-Cr<sub>2</sub>AlC composites were fabricated and tested for the first time by hot pressing. The addition of MAX Phase particulates enhanced the hardness and compressive yield strength of all the compositions. The yield strength is increased gradually from ~118 MPa in pristine Al to ~194 MPa in Al-30%V<sub>2</sub>AlC. Furthermore, the addition of Ti<sub>3</sub>SiC<sub>2</sub> and Cr<sub>2</sub>AlC increased the yield point gradually and reached to ~194 MPa and 211 MPa for the Al-30%Ti<sub>3</sub>SiC<sub>2</sub> and Al-30%Cr<sub>2</sub>AlC, respectively. In other words, the addition of 30% MAX phase particulates showed an enhancement in strength of ~1.7 times. The study showed that the addition of MAX phase particulates also had a remarkable effect on tribological performance. All the samples were tested by block (tab)-on-disk method. The pure Al samples showed  $\mu_{\text{mean}}$  value of 0.55. However, the addition of V<sub>2</sub>AlC and Ti<sub>3</sub>SiC<sub>2</sub> particulates decreased  $\mu_{\text{mean}}$  to below than 0.50. In contrary, the addition of Cr<sub>2</sub>AlC increased  $\mu_{\text{mean}}$  and same effect was also observed when Cr<sub>2</sub>AlC particulates were added to bismuth matrix. On the other hand, the WR of Al decreased



from  $0.25 \text{ mm}^3/\text{N.m}$  to  $1.1 \times 10^{-3} \text{ mm}^3/\text{N.m}$  in Al-30%V<sub>2</sub>AlC. Similarly, the addition of Ti<sub>3</sub>SiC<sub>2</sub> decreased the WR to  $7.3 \times 10^{-4} \text{ mm}^3/\text{N.m}$  in the Al-10%Ti<sub>3</sub>SiC<sub>2</sub>, thereafter it increased to  $1.6 \times 10^{-3} \text{ mm}^3/\text{N.m}$  and  $2.1 \times 10^{-3} \text{ mm}^3/\text{N.m}$  in the Al-20%Ti<sub>3</sub>SiC<sub>2</sub> and Al-30%Ti<sub>3</sub>SiC<sub>2</sub>, respectively. The addition of Cr<sub>2</sub>AlC at different concentrations retained almost similar WR values  $\sim(8-10) \times 10^{-4} \text{ mm}^3/\text{N.m}$ .

## CHAPTER V

### Conclusion and Future Scope

#### 5.1 Conclusion

Throughout this thesis, different MAX Reinforced Metals (MRMs) composites were studied for their mechanical and tribological behavior for the first time. The addition of MAX phase particulates has many beneficial effects on the mechanical and tribological behavior of MRMs. Although the porosity increased as the concentration of MAX phase content increased, the yield strength and wear resistance improved in all systems. Literature demonstrated that MAX phases exhibit outstanding tribological behavior at high temperatures compared to room temperatures. This work, along with the previous work at Advanced Material Science Lab at the University of North Dakota, showed a practical and beneficial effect of using these materials as particles reinforcement for soft metal matrix.

These studies confirm that the tribological behavior in a solid lubricant such as Ag can be further improved by adding MAX phase particulates in the matrix. In addition,  $Ti_3SiC_2$  showed remarkable effect in improving densification of Ag samples in pressure less sintering. Bismuth, the green alternative for lead, showed excellent performance when  $Ti_3SiC_2$  or  $Cr_2AlC$  particulates were added to it. The wear rate was decreased by more than ~60 times when 10% of  $Ti_3SiC_2$  is added to Bi. Furthermore, the yield strength and hardness were increase comparing with the pristine samples. The addition of  $Ti_3SiC_2$  particulates do not have a drastic effect of the grain size. The grain sizes were almost similar when the etched surfaces of Bi and Bi-20% $Ti_3SiC_2$ , Ag and Ag-20% $Ti_3SiC_2$  were investigated. Al-based composites showed also a significant improvement in tribological

behavior when MAX phases are added to the matrix. Al-Ti<sub>3</sub>SiC<sub>2</sub> and Al-Cr<sub>2</sub>AlC composites showed the same behavior in increasing porosity. However, Al-V<sub>2</sub>AlC did not affect porosity as the V<sub>2</sub>AlC is relatively softer than Ti<sub>3</sub>SiC<sub>2</sub> and Cr<sub>2</sub>AlC. The addition of MAX phase particulates also decreased  $\mu_{\text{mean}}$  compared with the pristine Al. Furthermore, the wear rate decreased significantly for Al-V<sub>2</sub>AlC and Al-Ti<sub>3</sub>SiC<sub>2</sub> composites compared to the pure Al. Wear rate decreased as the concentration of V<sub>2</sub>AlC increased in the Al-V<sub>2</sub>AlC. However, the addition of Ti<sub>3</sub>SiC<sub>2</sub> decreased the WR to  $7.3 \times 10^{-4}$  mm<sup>3</sup>/N.m in the Al-10%Ti<sub>3</sub>SiC<sub>2</sub>, thereafter it increased slightly in the Al-20%Ti<sub>3</sub>SiC<sub>2</sub> and Al-30%Ti<sub>3</sub>SiC<sub>2</sub>.

Many factors are affecting the mechanical and tribological behavior of MRMs composites. Presence of porosity in the sample affects the mechanical performance of the composites and could cause a reduction in hardness readings. Furthermore, some samples showed brittle failure during the compressive testing and the nature of failure should be studied for further analysis. Finally, it's always true that the addition of MAX phases improves the tribological behavior but there is an optimum concentration where the best results is found. That is mainly due to the nature of these phases where they perform much better at higher temperatures rather than room temperature.

## 5.2 Future Work

All the preceding work was done by using pure metals as matrix. The next level would be studying the effect of adding MAX phases to commercial metal alloys like aluminum-based alloys. The presented studies in this thesis worked with different MAX phases, namely Ti<sub>3</sub>SiC<sub>2</sub>, V<sub>2</sub>AlC and Cr<sub>2</sub>AlC. It would be recommended to study other phases like Cr<sub>2</sub>GaC to have better and comprehensive understanding about different MRMs.

Furthermore, as the science is moving toward nanotechnology, it would be recommended to study several systems in submicron size and report the effect as a function of particle sizes. Another approach would be depositing MRMs on the surface of stronger materials for improving tribocontact and improving their tribological behavior.

## References:

### Chapter I

1. "Modern tribology handbook, ch.22 Solid Lubricants and Self-Lubricating Films", B. Bhushan, Boca Raton, FL: CRC Press, 2001.
2. "Soft Metal Bearing Materials", W. Glaeser, Materials for tribology, Amsterdam, NY: Elsevier Science, 1992, pp. 69–88.
3. Friction and wear of materials. E. Rabinowicz, New York: John Wiley & sons, 1995.
4. "On the tribology of the MAX phases and their composites during dry sliding: A review", S. Gupta and M. Barsoum, Wear, vol. 271, no. 9-10, pp. 1878–1894, 2011.
5. "Synthesis and Characterization of Novel Al-Matrix Composites Reinforced with  $Ti_3SiC_2$  Particulates", S. Gupta, T. Hammann, R. Johnson, and M. F. Riyad, Journal of Materials Engineering and Performance, vol. 24, no. 2, pp. 1011–1017, Apr. 2014.
6. "Effect of  $Ti_3SiC_2$  Particulates on The Mechanical and Tribological Behavior of Sn Matrix Composites", T. Hammann, R. Johnson, M. F. Riyad, and S. Gupta, Advanced Processing and Manufacturing Technologies for Nanostructured and Multifunctional Materials II Ceramic Engineering and Science Proceedings, pp. 65–74, 2015.
7. "Synthesis and Characterization of  $Ti_3SiC_2$  Particulate-Reinforced Novel Zn Matrix Composites", S. Gupta, M. A. Habib, R. Dunnigan, N. Kaabouch, and S. Ghosh, Journal of Materials Engineering and Performance, vol. 24, no. 10, pp. 4071–4076, Mar. 2015.
8. "The  $M_{n+1}AX_n$  phases: A new class of solids", M. W. Barsoum, Progress in Solid State Chemistry, vol. 28, no. 1-4, pp. 201–281, 2000.
9. "Synthesis and Characterization of a Remarkable Ceramic:  $Ti_3SiC_2$ ", M. W. Barsoum and T. El-Raghy, Journal of the American Ceramic Society, vol. 79, no. 7, pp. 1953–1956, 1996.
10. "Tribological Properties of  $Ti_3SiC_2$ ", D. Sarkar, B. Basu, S. J. Cho, M. C. Chu, S. S. Hwang, and S. W. Park, Journal of the American Ceramic Society, vol. 88, no. 11, pp. 3245–3248, 2005.
11. "Tribology of MAX Phases and their composites", S. Gupta, PhD thesis, Drexel University (2006).
12. "Tribological Behavior of Novel  $Ti_3SiC_2$  (Natural Nanolaminates)-Reinforced Epoxy Composites during Dry Sliding", S. Gupta, T. Hammann, R. Johnson, and M. F. Riyad, Tribology Transactions, vol. 58, no. 3, pp. 560–566, 2015.

13. "The MAX Phases: Unique New Carbide and Nitride Materials", M. Barsoum and T. El-Raghy, *American Scientist*, vol. 89, no. 4, p. 334, 2001.

## Chapter II

1. "On the tribology of the MAX phases and their composites during dry sliding: A review", S. Gupta and M.W. Barsoum, *Wear* 271, 1878–1894 (2011).
2. "Applications of solid lubricant films in spacecraft", M. R. Hilton and P D Fleischauer, *Surface & coatings technology*, 54-55, 435–441 (1992).
3. "Ta<sub>2</sub>AlC and Cr<sub>2</sub>AlC Ag-based composites—New solid lubricant materials for use over a wide temperature range against Ni-based superalloys and alumina", S. Gupta, D. Filimonov, T. Palanisamy, T. El-Raghy, M.W. Barsoum, *Wear* 262, 1479–1489 (2007).
4. "Tribological and corrosive properties of silver thin films prepared by e-beam ion plating method", K-H Lee, O. Takai, M-H Lee, *Surface and Coatings Technology* 169 –170, 695–698 (2003).
5. "Tribological properties of silver coatings with laser surface textured nickel as interlayer", J. Li, Y. He, D. Xiong, Y. Qin, J. Chen, H. Zhu. *Tribology International* 100, 178–185 (2016).
6. "Adaptive VN/Ag nanocomposite coatings with lubricious behavior from 25 to 1000 °C", S.M. Aouadi, D.P. Singh, D.S. Stone, K. Polychronopoulou, F. Nahif, C. Rebholz, C. Muratore, A.A. Voevodin, *Acta Materialia*, 58, 5326-5331 (2010).
7. "Space tribological properties of metal matrix space lubricant coating prepared on titanium surface", C. Guo, R. Yao, H. Kong, J. Chen, J. Zhou, *Surface & Coatings Technology* 246, 40–45 (2014).
8. "Thrust-washer evaluation of self-lubricating PS304 composite coatings in high temperature sliding contact", T.A. Blanchet, J.H. Kim, S.J. Calabrese, C. Dellacorte, *Tribol. Trans.* 45, 491–498 (2002).
9. "Influence of silver content on the tribomechanical behavior on Ag-TiCN bioactive coatings", J.C. Sánchez-López, M.D. Abad, I. Carvalho, R. E. Galindo, N. Benito, S. Ribeiro, M. Henriques, A. Cavaleiro, S. Carvalho, *Surface & Coatings Technology* 206, 2192–2198 (2012).
10. "Bismuth – the new ecologically green metal for modern lubricating engineering", O. Rohr, *Industrial Lubrication and Tribology* 54,153 – 164 (2002).

11. "Tribiochemistry of Bismuth and Bismuth Salts for Solid Lubrication", P. Gonzalez-Rodriguez, K. J. H. van den Nieuwenhuijzen, W. Lette, D. J. Schipper, and J. E. ten Elshof, *ACS Appl. Mater. Interfaces* 8, 7601–7606 (2016).
12. "Tribological performance of some solid lubricants for hot forming through laboratory simulative tests", A. Tomala, S. Hernandez, M. Rodriguez Ripoll, E. Badisch, B. Prakash, *Tribology International* 74, 164–173 (2014).
13. "MAX Phases: Properties of Machinable Ternary Carbides and Nitrides", M.W. Barsoum, John Wiley & Sons (2013).
14. "Elastic and Mechanical Properties of the MAX Phases", M.W. Barsoum and M. Radovic *Annu. Rev. Mater. Res.* 41, 195-227 (2011).
15. "Synthesis and characterization of a remarkable ceramic:  $Ti_3SiC_2$ ", M.W. Barsoum, T. El-Raghy, *J. Am. Ceram. Soc.* 79, 1953–1956 (1996).
16. M.W. Barsoum, The  $M_{n+1}AX_n$  phases: a new class of solids; thermodynamically stable nanolaminates, *Prog. Solid State Chem.* 28, 201–281 (2000).
17. S. Amini, M.W. Barsoum, T. El-Raghy, Synthesis and mechanical properties of fully dense  $Ti_2SC$ , *J. Am. Ceram. Soc.* 90 (12), 3953–3958 (2007).
18. "Cu/ $Ti_3SiC_2$  composite: a new electrofriction material", Y. Zhang, Z.M. Sun, Y.C. Zhou, *Mater. Res. Innov.* 3, 80–84 (1999).
19. "Nanocrystalline Mg-matrix composites with ultrahigh damping properties", B. Anasori, S. Amini, V. Presser, and M. W. Barsoum, *Magnesium Technology*, John Wiley and Sons, Inc, 463-468 (2011).
20. "Powder metallurgy processing and compressive properties of  $Ti_3AlC_2/Al$  composites", W.J. Wang, V. Gauthier-Brunet, G.P. Bei, G. Laplanche, J. Bonneville, A. Joulain, S. Dubois, *Mater. Sci. Eng. A* 530, 168–173 (2011).
21. "Current-activated, pressure-assisted infiltration: a novel, versatile route for producing interpenetrating ceramic–metal composites", L. Hu, A. Kothalkar, M. O'Neil, I. Karaman, M. Radovic, *Mater. Res. Lett.* (2014)
22. "Thermo-mechanical response and damping behavior of shape memory alloy/MAX phase composites", A. Kothalkar, R. Benitez, L. Hu, M. Radovic, I. Karaman, *Metall. Mater. Trans. A.* 45, 2646–2658 (2014).
23. "Stability of  $V_2AlC$  with Al in 800-1000 °C temperature range and in situ synthesis of  $V_2AlC/Al$  composites", M.T. Agne, M. Radovic, G.W. Bentzel, M.W. Barsoum, *J. Alloys Compd.*, 666, 279-286 (2016)

24. "Synthesis and Characterization of Novel Al-Matrix Composites Reinforced with  $Ti_3SiC_2$  Particulates", S. Gupta, T. Hammann, R. Johnson, and M.F. Riyad, *Journal of Materials Engineering and Performance*, 24, 1011-1017 (2014).
25. "Novel  $Ti_3SiC_2$  reinforced Sn matrix composites", T. Hammann, R. Johnson, M. F. Riyad, and S. Gupta, *Proceedings of 39th Int'l Conf & Expo on Advanced Ceramics & Composites (ICACC 2015)*.
26. "Synthesis and Characterization of  $Ti_3SiC_2$  Particulate-Reinforced Novel Zn Matrix Composites", S. Gupta, Habib, M.A., Dunnigan, R. et al. *J. of Materi Eng and Perform* (2015) 24: 4071.
27. "NIH Image to ImageJ: 25 years of image analysis", C. A Schneider, W. S Rasband, & K. W. Eliceiri, *Nature Methods*, 9, 671–675 (2012).
28. "Nickel assisted sintering of  $Ti_3SiC_2$  powder under pressureless conditions", B. B. Panigrahi, N. S. Reddy, A. Balakrishnan, M. Chu, S. Cho, J. J. Gracio, *J. Alloys Compd.*, 505, 337– 342 (2010).
29. *Tribology of MAX Phases and their composites*", S. Gupta, PhD thesis, Drexel University (2006).

### Chapter III

1. "Bismuth – the new ecologically green metal for modern lubricating engineering", O. Rohr, *Industrial Lubrication and Tribology* 54,153 – 164 (2002).
2. "Tribochemistry of Bismuth and Bismuth Salts for Solid Lubrication", P. Gonzalez-Rodriguez, K. J. H. van den Nieuwenhuijzen, W. Lette, D. J. Schipper, and J. E. ten Elshof, *ACS Appl. Mater. Interfaces* 8, 7601–7606 (2016).
3. "Synthesis and Tribological Behavior of Novel Ag- and Bi-based Composites Reinforced with  $Ti_3SiC_2$  ", F. AlAnazi, S. Ghosh, R. Dunnigan, and S. Gupta (accepted for publication in *Wear*).
4. "MAX Phases: Properties of Machinable Ternary Carbides and Nitrides", M.W. Barsoum, John Wiley & Sons (2013).
5. "Elastic and Mechanical Properties of the MAX Phases", M.W. Barsoum and M. Radovic *Annu. Rev. Mater. Res.* 41, 195-227 (2011).
6. "Synthesis and characterization of a remarkable ceramic:  $Ti_3SiC_2$ ", M.W. Barsoum, T. El-Raghy, *J. Am. Ceram. Soc.* 79, 1953–1956 (1996).



7. M.W. Barsoum, The  $M_{n+1}AX_n$  phases: a new class of solids; thermodynamically stable nanolaminates, *Prog. Solid State Chem.* 28, 201–281 (2000).
8. S. Amini, M.W. Barsoum, T. El-Raghy, Synthesis and mechanical properties of fully dense  $Ti_2SC$ , *J. Am. Ceram. Soc.* 90 (12), 3953–3958 (2007).
9. “Synthesis and Characterization of Novel Al-Matrix Composites Reinforced with  $Ti_3SiC_2$  Particulates”, S. Gupta, T. Hammann, R. Johnson, and M.F. Riyad, *Journal of Materials Engineering and Performance*, 24, 1011-1017 (2014).
10. “Effect of  $Ti_3SiC_2$  Particulates on The Mechanical and Tribological Behavior of Sn Matrix Composites”, T. Hammann, R. Johnson, M. F. Riyad, and S. Gupta, *Proceedings of 39th Int'l Conf & Expo on Advanced Ceramics & Composites (ICACC 2015)*.
11. “Synthesis and Characterization of  $Ti_3SiC_2$  Particulate-Reinforced Novel Zn Matrix Composites”, S. Gupta, Habib, M.A., Dunnigan, R. et al. *J. of Materi Eng and Perform* (2015) 24: 4071.
12. “On the tribology of the MAX phases and their composites during dry sliding: A review”, S. Gupta and M.W. Barsoum, *Wear* 271, 1878– 1894 (2011).
13. “Tribology of MAX Phases and their composites”, S. Gupta, PhD thesis, Drexel University (2006).

## Chapter IV

1. "Influences of graphite reinforcement on the tribological properties of self-lubricating aluminum matrix composites for green tribology, sustainability, and energy efficiency—a review ", E. Omrani, et al. *Int J Adv Manuf Technol*, vol. 83, no. 1-4, pp. 325–346, 2016
2. “Synthesis and Characterization of Novel Al-Matrix Composites Reinforced with  $Ti_3SiC_2$  Particulates”, S. Gupta, T. Hammann, R. Johnson, and M.F. Riyad, *Journal of Materials Engineering and Performance*, 24, 1011-1017 (2014).
3. “Effect of  $Ti_3SiC_2$  Particulates on The Mechanical and Tribological Behavior of Sn Matrix Composites”, T. Hammann, R. Johnson, M. F. Riyad, and S. Gupta, *Proceedings of 39th Int'l Conf & Expo on Advanced Ceramics & Composites (ICACC 2015)*.
4. “Synthesis and Characterization of  $Ti_3SiC_2$  Particulate-Reinforced Novel Zn Matrix Composites”, S. Gupta, Habib, M.A., Dunnigan, R. et al. *J. of Materi Eng and Perform* (2015) 24: 4071.
5. “Effect of graphite particle reinforcement on dry sliding wear of SiC/Gr/Al composites”, L. Jinfeng, et al., *Rare Metal Materials and Engineering*, vol. 38, no. 11, pp. 1894–1898, 2009

6. Tribology of MAX Phases and their composites”, S. Gupta, PhD thesis, Drexel University (2006).
7. “Friction and Wear of Aluminum Matrix Composites”, M. Kozma, National Tribology Conference 24-26 September 2003
8. “Functional Metal Matrix Composites: Self-lubricating, Self-healing, and Nanocomposites- An Outlook,” A. D. Moghadam, et al., *Jom*, vol. 66, no. 6, pp. 872–881, May 2014.
9. “Correlation between the characteristics of the mechanically mixed layer and wear behaviour of aluminum, Al-7075 alloy and Al-MMCs”, B. Venkataraman and G. Sundararajan, *Wear*, vol. 245, no. 1-2, pp. 22–38, 2000.
10. “MAX Phases: Properties of Machinable Ternary Carbides and Nitrides”, M.W. Barsoum, John Wiley & Sons (2013).
11. “Elastic and Mechanical Properties of the MAX Phases”, M.W. Barsoum and M. Radovic *Annu. Rev. Mater. Res.* 41, 195-227 (2011).
12. “Synthesis and characterization of a remarkable ceramic:  $Ti_3SiC_2$ ”, M.W. Barsoum, T. El-Raghy, *J. Am. Ceram. Soc.* 79, 1953–1956 (1996).
13. M.W. Barsoum, The  $M_{n+1}AX_n$  phases: a new class of solids; thermodynamically stable nanolaminates, *Prog. Solid State Chem.* 28, 201–281 (2000).
14. “On the tribology of the MAX phases and their composites during dry sliding: A review”, S. Gupta and M.W. Barsoum, *Wear* 271, 1878– 1894 (2011).
15. “In Situ Reaction Synthesis and Mechanical Properties of  $V_2AlC$ ” C. Hu, et al., *Journal of the American Ceramic Society*, vol. 91, no. 12, pp. 4029–4035, 2008.
16. “Synthesis and Tribological Behavior of Novel Ag- and Bi-based Composites Reinforced with  $Ti_3SiC_2$ ”, F. AlAnazi, S. Ghosh, R. Dunnigan, and S. Gupta (accepted for publication in *Wear*).